processes

MDPI

Review

Opportunities and Constraints of the Adsorption of Rare Earth Elements onto Pyrolytic Carbon-Based Materials: A Mini-Review

Miguel Nogueira [1], Maria Bernardo [1], Márcia Ventura [1], Inês Matos [1], Filomena Pinto [2] and Nuno Lapa [1,*]

[1] LAQV-REQUIMTE, Associated Laboratory for Green Chemistry, Department of Chemistry, NOVA School of Science and Technology, NOVA University Lisbon, 2829-516 Caparica, Portugal; mf.nogueira@campus.fct.unl.pt (M.N.); maria.b@fct.unl.pt (M.B.); mm.ventura@fct.unl.pt (M.V.); ines.matos@fct.unl.pt (I.M.)

[2] UBB-LNEG, Unidade de Bioenergia e Biorrefinarias, Laboratório Nacional de Energia e Geologia, 1649-038 Lisboa, Portugal; filomena.pinto@lneg.pt

* Correspondence: ncsn@fct.unl.pt

Abstract: Rare earth elements (REEs), comprising seventeen metallic elements, including lanthanides, scandium, and yttrium, are indispensable for modern technological industries due to their unique properties. However, their supply is critically risky for the European Union, with 95% of global production concentrated in China, Brazil, Vietnam, Russia, India, and Australia. This mini-review examines the adsorption of REEs onto pyrolytic carbon-based materials as a sustainable recovery method from secondary raw materials. The review covers different types of carbon-based adsorbents used in several research works, such as activated carbon, chars, and biochar, and discusses their adsorption mechanisms and influencing factors. Comparative analyses of adsorption capacities highlight the significance of surface area and functionalization in enhancing adsorption efficiency. Despite promising results, the variability in adsorption performance due to experimental conditions and the scarcity of real-world application studies are noticed. This review underscores the need for further research using real e-waste leachates to validate the practical applicability of pyrolytic carbon-based adsorbents for REEs' recovery, aiming for an economically and environmentally sustainable solution.

Keywords: rare earth elements; adsorption; carbon materials; recovery; chars; activated carbons

Citation: Nogueira, M.; Bernardo, M.; Ventura, M.; Matos, I.; Pinto, F.; Lapa, N. Opportunities and Constraints of the Adsorption of Rare Earth Elements onto Pyrolytic Carbon-Based Materials: A Mini-Review. *Processes* **2024**, *12*, 2257. https://doi.org/10.3390/pr12102257

Academic Editor: Maria Josè Lo Faro

Received: 9 September 2024
Revised: 29 September 2024
Accepted: 15 October 2024
Published: 16 October 2024

1. Introduction

Rare earth elements (REEs) are a group of seventeen metallic elements with chemical similarities, which include the lanthanide series (La, Ce, Pr, Nd, Pm, Sm, Eu, Gd, Tb, Dy, Ho, Er, Tm, Yb, and Lu), as well as Sc and Y. These elements are critical raw materials (CRMs) for the technological industry in Europe and worldwide [1–3].

In its latest report on Critical Raw Materials for the European Union (EU), the European Commission identified REEs as the most critical group (Figure 1), due to the highest supply risk [1]. This was also recognized by the United States Department of Energy in their Critical Materials Strategy [2,3]. The most critical REEs are dysprosium (Dy), europium (Eu), neodymium (Nd), terbium (Tb), and yttrium (Y) [4].

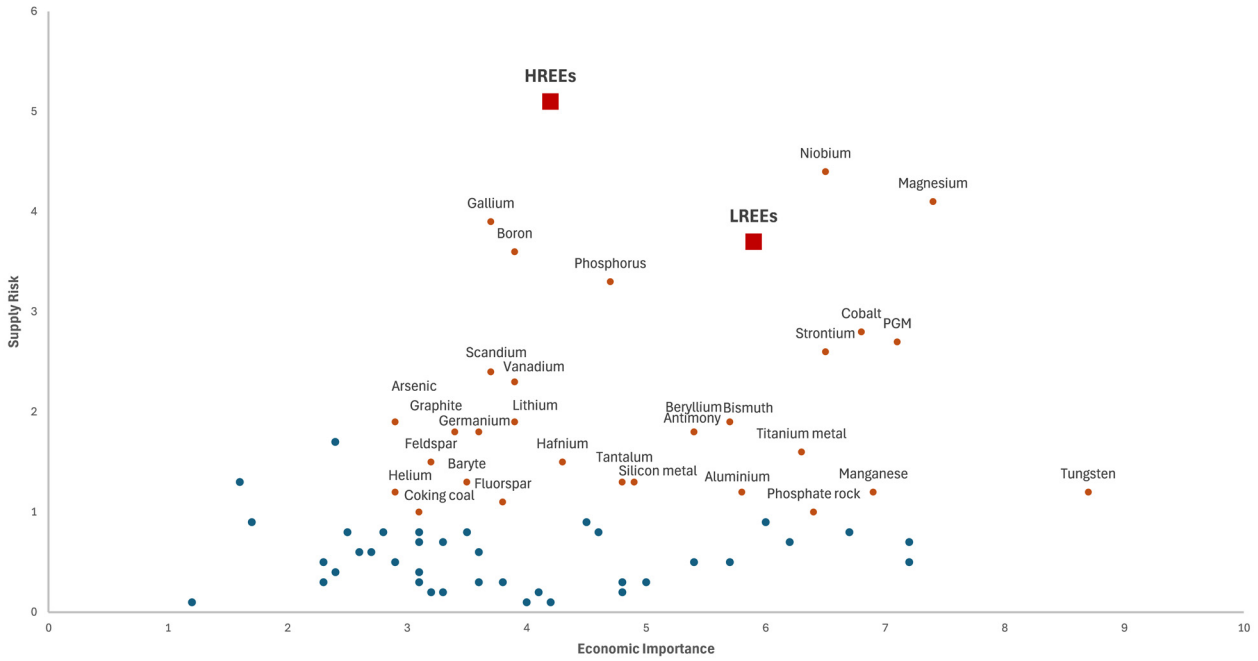

Figure 1. Economic importance and supply risk of CRM; REEs highlighted by red square markers; Blue dots—Materials that lost CRM status; LREEs—light rare earth elements; HREEs—heavy rare earth elements; adapted and sourced from [1,5].

REEs do not occur in nature as individual native metals due to their reactivity but instead exist together in various ores and minerals, typically as minor constituents. Although REEs can be found in a wide variety of minerals and ores, they are confined to specific geological environments. This creates a problem for the supply risk level, as most REEs' deposits are concentrated in a small group of countries, including China, Brazil, Vietnam, Russia, India, and Australia [6]. Other reserves are scattered globally but account for less than 1% of total world reserves. Currently, China produces nearly 80% of the global REE demand, followed by Australia, with 15%, reinforcing the supply risk in Europe and the USA, as 95% of production is met by just these two countries [4,6,7].

Table 1 highlights the importance of REEs due to their wide applicability in different technologies and industrial sectors.

Table 1. Overview of major REE applications by industrial sector. Adapted and sourced from [1,6,8].

Industrial Sector	Applications
Technology	Permanent magnets, lasers, optical glass, fiber optics, masers, radar detection devices, nuclear fuel rods, mercury vapor lamps, highly reflective glass, computer memory, nuclear batteries, and high-temperature superconductors
Electronics	TV screens, computers, cell phones, silicon chips, monitor displays, long-life rechargeable batteries, camera lenses, light-emitting diodes (LEDs), compact fluorescent lamps (CFLs), scanners, and propulsion systems
Medical sector	Portable X-ray machines, X-ray tubes, magnetic resonance imagery, contrast agents, nuclear medicine imaging, cancer treatment applications, and genetic screening tests
Renewable energy	Hybrid automobiles, wind turbines, rechargeable batteries, biofuel catalysts, hydrogen storage, and fuel cells
Diverse manufacturing sectors	High-strength magnets, metal alloys, stress gauges, ceramic pigments, colorants, chemical oxidizing agents, polishing powders, polymer production, metal alloy strengthening-additive, and automotive catalytic converters

REEs play an increasingly vital role in the transition to a sustainable, low-carbon, and low-environmental-impact economy due to their unique magnetic, catalytic, and phosphorescent properties. These properties make them critical resources for a wide range of high-technology industries (Table 1), such as cell phones, televisions, and lamp phosphors, as well as wind turbines and electric vehicles [6,7,9].

The EU has identified CRMs as materials of high economic and strategic importance for its economy, with significant supply risks. CRMs are not considered critical due to scarcity but rather for their economic importance in key sectors, high supply risk due to the EU's reliance on foreign sources, and the absence of viable substitutes due to their unique properties and applications. The EU's list of 51 CRMs includes REEs, highlighting their critical nature [1].

To secure a sustainable supply of REEs, the EU must ensure a steady flow of these materials and support high-tech industries and research centers in finding solutions [9–11]. This can be achieved through several approaches: diversifying and globalizing supply chains, establishing new bilateral trade agreements, planning strategic reserves, adopting more sustainable and economical extraction methods, increasing resource efficiency, and promoting research initiatives [12]. In this context, developing pathways to recycle and reuse CRMs, such as extracting precious materials from Waste Electrical and Electronic Equipment (WEEE), is of particular relevance [1,9–11,13].

Pyrolytic carbon-based materials have surfaced as highly promising adsorbents for the recovery of REEs from secondary raw materials, attributed to their specific properties, versatility, and cost-effectiveness [8,9]. These materials, in which activated carbon, chars, and biochars are included, possess high surface areas, abundant pore structures, and a wide array of functional groups that promote the adsorption of REEs [8,14]. The porous structure of these materials allows for a higher contact area that can interact with REE ions, increasing their adsorption capacity [15]. Moreover, these adsorbents can be derived from a variety of low-cost and sustainable sources, for instance, wastes, biowastes, biomass, and other industrial by-products, which promote these materials as environmentally and economically sustainable options for large-scale applications [16–18].

Activated carbons are produced by the pyrolysis of carbonaceous matrices followed by an activation step (either physical or chemical) in which the morphology of the structure is further developed, resulting in increased surface areas [19]. They have been widely studied for their excellent adsorption capacities [20]. Similarly, biochar and chars, which are yielded through the pyrolysis of biomass under inert atmosphere conditions, offer potential advantages due to their environmental benefits and lower production costs [18,21,22]. The presence of functional groups on these adsorbents' surface, such as carboxyl, hydroxyl, and phenolic groups, as well as their mineral content, play a pivotal part in the adsorption of REE ions [21,23–26]. These materials not only sequester carbon but also provide a sustainable method for waste management through their economic added value.

Given the critical need for resource recovery and the practical challenges associated with the production and application of advanced carbon materials, this review focuses on the adsorption of REEs using chars, activated carbons, and other simpler carbon materials. By "simpler carbon materials", we refer to those that are more readily available and cost-effective, typically derived from biomass or other inexpensive precursors, and require less complex production processes compared to advanced materials like carbon nanotubes (CNTs), fullerenes, and graphene. This focus aligns better with the objectives of sustainable resource recovery, emphasizing practical and scalable solutions for REE recovery. By excluding more complex and harder-to-produce materials, the review ensures broader applicability and feasibility in industrial processes. Nevertheless, some of these advanced materials will be analyzed for comparison purposes.

This mini-review aims to provide a comprehensive overview of the current state of research on the adsorption of REEs onto pyrolytic carbon-based materials. Specifically, it will (i) evaluate the types of carbon-based adsorbents used for REE recovery, including activated carbon, chars, and biochar; (ii) analyze the adsorption mechanisms and factors

influencing adsorption efficiency; (iii) compare adsorption capacities of different carbon-based materials; (iv) highlight the challenges and limitations in current research, especially the variability in experimental conditions and the scarcity of real-world application studies; and (v) suggest future research directions to enhance the practical applicability of pyrolytic carbon-based adsorbents for sustainable and efficient REE recovery. To ensure a representative review, a systematic search of the available literature was performed. The search covered publications from 2000 to 2024, using key terms such as (i) rare earth elements, (ii) carbon-based materials, (iii) REE adsorption, (iv) REE recovery, (v) chars, (vi) biochar, and (vii) activated carbon. The consulted databases were (i) Scopus, (ii) Web of Science, (iii) Google Scholar, and (iv) PubMed.

By addressing these objectives, this review seeks to underline the potential of pyrolytic carbon-based materials in contributing to a sustainable solution for REE recovery and to encourage further research in this field.

2. Adsorption of Rare Earth Elements

The adsorption of REEs is scarcely reported in the literature [8,15,26]. Specifically, studies on the adsorption of these metals onto porous carbon materials are even rarer, with only a few available papers addressing this topic. Reports on the competitive adsorption and dynamic adsorption of these lanthanides are even fewer.

Although adsorption processes can be considered sustainable and green, the type and nature of the used adsorbent play a crucial role in the economic and environmental feasibility of this process. This review focuses on the adsorption of REEs onto waste-derived chars, activated carbons, and other simpler carbon materials to maintain a sustainable approach to tackling the problem at hand. Beyond carbon-based materials, other types of adsorbents have been studied in the context of REE recovery or adsorption. Examples of these materials include metal-organic frameworks, zeolites, clays, ion-exchange resins, and composite materials [8,15,27]. Research on these materials offers alternative insights into adsorption processes, with each being investigated for REE recovery in specialized applications.

Table 2 presents a summary of the current progress made toward the adsorption of REEs using these carbon-based materials. This review highlights the importance of these materials in promoting sustainable resource recovery, providing insights into their adsorption capacities and practical applications.

Table 2. Adsorption of REEs using carbon-based materials.

Adsorbent	Type of Adsorption Assay	Tested REE	Max. Adsorption Capacity ($mg \cdot g^{-1}$)	Recovery Capacity (%)	S_{BET} ($m^2 \cdot g^{-1}$)	pH	Temperature (K)	Ref.
Functionalized lignin-activated carbon	Batch	Nd	335.5	100	837	2, 4, 6	Room	[28]
Functionalized lignin-activated carbon		Dy	344.6	100	837			
Spent coffee physical-activated carbon	Batch	Dy	33.52	100	2330	3–5	303, 318, 333	[29]
Spent coffee chemical-activated carbon			31.26	100	982			
Commercial activated carbon	Batch	Nd	36.65	73	980	-	293	[30]
Multi-wall carbon nanotubes from crystalline nanocellulose	Batch	Dy	48.14	100	-	2–7	290, 298, 208	[31]
Sawdust biochar	Batch	Nd	8.0	40	4.7	3	Room	[32]
		Sc	7.5	38				
Commercial activated carbon (CAC)		Nd	8.8	44	912			
		Sc	8.5	42				

Table 2. *Cont.*

Adsorbent	Type of Adsorption Assay	Tested REE	Max. Adsorption Capacity ($mg \cdot g^{-1}$)	Recovery Capacity (%)	S_{BET} ($m^2 \cdot g^{-1}$)	pH	Temperature (K)	Ref.
Carbon black from recycled tires	Batch	Nd La Ce Sm Y	0.54 0.34 0.70 0.55 0.46	-	57	-	298, 313, 333, 353	[33]
Commercial activated carbon (CAC) Oxidized CAC EDTA Functionalized oxidized CAC	Batch	Nd	19.1 50.8 71.4	-	711 761 741	5	293	[34]
Oxidized carbon nanofibers	Column	La Eu Gd Yb	18.1 17.6 14.2 19.1	-	-	1–7	-	[35]
PAN-grafted carbon nanotubes–silica	Batch	La Sc Y	103.5 112.7 84.1	-	107	1–6	296, 318	[36]
Carbon xerogel–chitosan composite	Batch		163.9	-	275	0.5–6	298	[37]
Carbon nanoparticles	Batch	Nd La	0.45 0.51	99 99	1800	3	293	[38]
PAM-activated carbon composite	Batch	Nd Ce Gd	9.88 9.61 9.26	-	-	-	298	[39]
Commercial activated carbon $KMnO_4$-modified commercial activated carbon	Batch	La Yb Lu Eu Y Sc La Yb Lu Eu Y Sc	0.048 0.053 0.052 0.038 0.057 0.069 0.071 0.084 0.075 0.097 0.089 0.121	- -	381 346	2–8	298	[40]
Oligo-grafted synthetic mesoporous carbon	Batch	Lu Dy La	9.57 38.27 52.15	-	-	-	-	[41]
Commercial activated carbon graphene oxide nanosheets	Batch	Eu	20.0 161.3	-	- 120	2–11	298	[42]
Commercial activated carbon Carbon nanotubes Graphite oxide	Batch	Sc	2.1 37.9 36.5	-	405 227 175	1–6	Room	[43]
Apricot stone char Activated carbon (H_3PO_4 activation) Activated carbon (KOH activation)	Batch	Eu	17.8 29.3 28.4	-	100 554 98	2–8	293, 313, 333	[25]
Schiff's base-modified activated carbon	Batch	La	144.8	-		1–7	Room	[24]
CMK-8 (ordered mesoporous carbon) Oxidized CMK-8 DGO-grafted CMK-8	Batch	Sm	3.31 22.3 9.83	-	914 933 439	2.6	-	[23]

Table 2. *Cont.*

Adsorbent	Type of Adsorption Assay	Tested REE	Max. Adsorption Capacity ($mg \cdot g^{-1}$)	Recovery Capacity (%)	S_{BET} ($m^2 \cdot g^{-1}$)	pH	Temperature (K)	Ref.
Spent tire-rubber char (A450)	Batch	Nd Dy	10.0 11.7	-	74	-	Room	[14]
Spent tire-rubber char (B450)		Nd Dy	12.5 13.1		73			
Spent tire-rubber char (A900)		Nd Dy	32.8 34.3		75			
Spent tire-rubber char (B900)		Nd Dy	28.2 32.8		73			
Commercial activated carbon		Nd Dy	12.8 10.8		1030			
Mesoporous carbon	Batch	La Dy Lu	2.0 1.8 1.6	-	594	-	-	[44]
Carboxylated mesoporous carbon		La Dy Lu	4.3 6.0 6.5		438			
Soybean pod-activated carbon	Batch	Ce La	107.7 127.2	-	614	1–6	298, 308, 318, 328	[45]
Wood-waste biochar	Batch	Ce	327.9	-	8.8	1–7	298, 308, 318, 328	[46]

Saha et al. investigated the adsorption of Nd and Dy using functionalized lignin AC. Their study demonstrated that the adsorption capacity for Nd was 335.5 $mg \cdot g^{-1}$, and for Dy, it was 344.6 $mg \cdot g^{-1}$. The functionalization enhanced the binding sites available for the REEs, resulting in superior adsorption performance. The material had a specific surface area (S_{BET}) of 837 $m^2 \cdot g^{-1}$ [28].

Alcaraz et al. explored the use of physically and chemically activated carbon from spent coffee grounds for the removal of Dy. Their study found that the physically activated carbon had an adsorption capacity of 33.52 $mg \cdot g^{-1}$ with an S_{BET} of 2330 $m^2 \cdot g^{-1}$, while the chemically activated carbon had an adsorption capacity of 31.26 $mg \cdot g^{-1}$ with an S_{BET} of 982 $m^2 \cdot g^{-1}$ [29].

Qadeer studied the adsorption of Nd by applying commercial activated carbon. The study found that the maximum uptake capacity for Nd was 36.65 $mg \cdot g^{-1}$ in the tested conditions, and the S_{BET} of the material was 980 $m^2 \cdot g^{-1}$ [30].

Zheng et al. investigated the adsorption of Dy using multi-wall CNTs derived from crystalline nano cellulose, which achieved an adsorption capacity of 48.14 $mg \cdot g^{-1}$ [31].

Komnitsas et al. studied the adsorption of Nd and Sc using sawdust biochar with an S_{BET} of 4.7 $m^2 \cdot g^{-1}$. The adsorption capacities were found to be 8.0 $mg \cdot g^{-1}$ for Nd and 7.5 $mg \cdot g^{-1}$ for Sc [32].

Smith et al. explored the adsorption of various REEs using carbon black derived from recycled tires with a surface area of 57 $m^2 \cdot g^{-1}$. The adsorption capacities were 0.54 $mg \cdot g^{-1}$ for Nd, 0.34 $mg \cdot g^{-1}$ for La, 0.70 $mg \cdot g^{-1}$ for Ce, 0.55 $mg \cdot g^{-1}$ for Sm, and 0.46 $mg \cdot g^{-1}$ for Y [33].

Babu et al. studied the adsorption of Nd using various forms of commercial activated carbons (CACs). The unmodified CAC showed an adsorption capacity of 19.1 $mg \cdot g^{-1}$, with an S_{BET} of 711 $m^2 \cdot g^{-1}$. When oxidized, the adsorption capacity increased to 50.8 $mg \cdot g^{-1}$, with an S_{BET} of 761 $m^2 \cdot g^{-1}$. The highest adsorption capacity was observed with EDTA-functionalized oxidized CAC (EDTA—ethylenediaminetetraacetic acid), which achieved 71.4 $mg \cdot g^{-1}$ and an S_{BET} of 741 $m^2 \cdot g^{-1}$. This progression indicates the significant impact of surface modification and functionalization on adsorption performance [34].

Chen et al. used oxidized carbon nanofibers for the adsorption of La, Eu, Gd, and Yb. The adsorption capacities were 18.1 $mg \cdot g^{-1}$ for La, 17.6 $mg \cdot g^{-1}$ for Eu, 14.2 $mg \cdot g^{-1}$ for Gd, and 19.1 $mg \cdot g^{-1}$ for Yb [35].

Ramasamy et al. investigated the adsorption of La, Sc, and Y using PAN (1-(2-pyridylazo)-2-naphthol)-grafted CNT–silica composites. The adsorption capacities were 103.5 $mg \cdot g^{-1}$ for La, 112.7 $mg \cdot g^{-1}$ for Sc, and 84.1 $mg \cdot g^{-1}$ for Y, with an S_{BET} of 107 $m^2 \cdot g^{-1}$ [36].

Haggag et al. developed a carbon xerogel–chitosan composite for the adsorption of REEs. The adsorption capacity was 163.9 $mg \cdot g^{-1}$, with an S_{BET} of 275 $m^2 \cdot g^{-1}$ [37].

Younis et al. investigated the adsorption of Nd and La using carbon nanoparticles with an S_{BET} of 1800 $m^2 \cdot g^{-1}$. The adsorption capacities were 0.45 $mg \cdot g^{-1}$ for Nd and 0.51 $mg \cdot g^{-1}$ for La [38].

El-Masry et al. studied the adsorption of Nd, Ce, and Gd using a PAM-activated carbon composite (PAM—polyacrylamide). The adsorption capacities were 9.88 $mg \cdot g^{-1}$ for Nd, 9.61 $mg \cdot g^{-1}$ for Ce, and 9.26 $mg \cdot g^{-1}$ for Gd [39].

Kano et al. investigated the adsorption of various REEs onto CAC modified with potassium permanganate (KMnO4). The study showed that the KMnO4 modification enhanced the adsorption capacities compared to unmodified CAC. For instance, the adsorption capacity for Sc increased from 0.069 $mg \cdot g^{-1}$ to 0.121 $mg \cdot g^{-1}$. Similarly, enhancements were observed for other REEs, such as La, Yb, Lu, Eu, and Y, demonstrating the effectiveness of KMnO4 modification in improving adsorption performance [40].

Gismondi et al. explored the adsorption of La, Dy, and Lu using oligo-grafted synthetic mesoporous carbon. The adsorption capacities were 52.15 $mg \cdot g^{-1}$ for La, 38.27 $mg \cdot g^{-1}$ for Dy, and 9.57 $mg \cdot g^{-1}$ for Lu [41].

Sun et al. investigated the adsorption of REEs using graphene oxide (GO) nanosheets. The adsorption capacity was 161.3 $mg \cdot g^{-1}$ [42].

Kilian et al. conducted a comparative study on the sorption of Sc onto various carbon-based materials. The adsorption capacity of CAC for Sc was found to be 2.1 $mg \cdot g^{-1}$, with an S_{BET} of 405 $m^2 \cdot g^{-1}$. Additionally, the study included CNTs and GOs, which showed significantly higher adsorption capacities of 37.9 $mg \cdot g^{-1}$ and 36.5 $mg \cdot g^{-1}$, respectively; however, these materials were not the primary focus due to their production complexities [43].

Gad and Awwad explored the factors affecting the sorption/desorption of Eu using various ACs. The apricot stone char exhibited an adsorption capacity of 17.8 $mg \cdot g^{-1}$, while activated carbons with H_3PO_4 and KOH activation showed capacities of 29.3 $mg \cdot g^{-1}$ and 28.4 $mg \cdot g^{-1}$, respectively. These findings underscore the importance of activation methods in enhancing the adsorption performance of carbon materials [25].

Marwani et al. studied the adsorption of La using Schiff's base-modified AC. The adsorption capacity was 144.8 $mg \cdot g^{-1}$ [24].

Perreault et al. investigated the adsorption of Sm using CMK-8, an ordered mesoporous carbon. The adsorption capacity was 3.31 $mg \cdot g^{-1}$, with an S_{BET} of 914 $m^2 \cdot g^{-1}$. Oxidized CMK-8 had an adsorption capacity of 22.3 $mg \cdot g^{-1}$, with an S_{BET} of 933 $m^2 \cdot g^{-1}$, and DGO (diglycolylester)-grafted CMK-8 had an adsorption capacity of 9.83 $mg \cdot g^{-1}$, with an S_{BET} of 439 $m^2 \cdot g^{-1}$ [23].

Nogueira et al. explored the use of pyrolytic carbon-based adsorbents derived from spent-tire rubber for the recovery of Nd and Dy. Their study investigated different char types produced at various temperatures. The spent tire-rubber char (A450) exhibited adsorption capacities of 10.0 $mg \cdot g^{-1}$ for Nd and 11.7 $mg \cdot g^{-1}$ for Dy, while char (B450) showed slightly higher capacities of 12.5 $mg \cdot g^{-1}$ for Nd and 13.1 $mg \cdot g^{-1}$ for Dy. Chars produced at higher temperatures, such as A900 and B900, demonstrated significantly enhanced adsorption capacities, with A900 adsorbing 32.8 $mg \cdot g^{-1}$ of Nd and 34.3 $mg \cdot g^{-1}$ of Dy, and B900 adsorbing 28.2 $mg \cdot g^{-1}$ of Nd and 32.8 $mg \cdot g^{-1}$ of Dy. These findings highlight the influence of pyrolysis temperature on the adsorption performance of carbon materials derived from waste rubber [14].

Saha et al. studied the adsorption performance of mesoporous carbon and a carboxylated version of the same material and observed that the carboxylated material adsorbed 2-to-4 times the quantities of REEs when compared with its pristine version. This investigation emphasized that although the carboxylated material had lower surface areas and pore volumes than the pristine mesoporous carbon, the enhancement of REE uptake was

undoubtedly caused by the carboxylate functionalization. They further evaluated the recovery of REEs from coal fly-ash leachates [44].

Pinheiro et al. studied the adsorption of Ce and La onto soybean pod AC. The material they produced was able to achieve maximum uptake capacities of 107.7 and 127.2 $mg \cdot g^{-1}$ for Ce and La, respectively. They also evaluated the recovery of these REEs from phosphogypsum leachate [45].

A wood-waste biochar produced via the hydrothermal carbonization of *Prunus serrulata* bark was studied for the adsorption of Ce by Reis et al. [46]. Although the material has a very low surface area (8.8 $m^2 \cdot g^{-1}$), it was able to reach uptake capacities of 327.9 $mg \cdot g^{-1}$ due to surface precipitation resulting from the REE interaction with OH and COOH functional groups, as well as surface complexation with hydroxyl groups on the biochar's surface. The material was also assayed for the recovery of Ce from phosphogypsum leachate [46].

The maximum adsorption capacities (Figure 2 and Table 2) of REEs on various carbon-based adsorbents fluctuate greatly depending on the surface area of the material, their mineral composition, the surface chemistry, and the presence of grafted or added compounds [27,47]. Functionalized lignin-activated carbon exhibits the highest adsorption capacities for Nd and Dy, with values of 335.5 $mg \cdot g^{-1}$ and 344.6 $mg \cdot g^{-1}$, respectively, and an S_{BET} of 837 $m^2 \cdot g^{-1}$. This high performance can be attributed to phosphorus functionalization, which enhances the binding sites available for REEs, leading to a superior adsorption performance [28,41].

In comparison, spent-coffee AC also shows high adsorption capacities, particularly when physically activated, with an adsorption capacity of 33.52 $mg \cdot g^{-1}$ for Dy and an exceptionally high S_{BET} of 2330 $m^2 \cdot g^{-1}$. However, the chemically activated version, while still effective with a capacity of 31.26 $mg \cdot g^{-1}$ for Dy, has a significantly lower S_{BET} of 982 $m^2 \cdot g^{-1}$. This demonstrates that a higher surface area alone does not necessarily correlate with a higher adsorption capacity, as the type of activation and presence of functional groups play crucial roles [29].

Carbon materials with specific modifications or grafting often show enhanced adsorption capacities. For instance, PAN-grafted CNT–silica composites show high capacities (103.5 $mg \cdot g^{-1}$ for La and 112.7 $mg \cdot g^{-1}$ for Sc), with an S_{BET} of 107 $m^2 \cdot g^{-1}$, illustrating the significant impact of grafting on adsorption performance despite a relatively lower surface area [36].

Carbon xerogel–chitosan composites and GO nanosheets also highlight the importance of functionalization [37,42]. The xerogel–chitosan composite has an adsorption capacity of 163.9 $mg \cdot g^{-1}$, with an S_{BET} of 275 $m^2 \cdot g^{-1}$, while GO nanosheets, with an S_{BET} of 120 $m^2 \cdot g^{-1}$, achieve an adsorption capacity of 161.3 $mg \cdot g^{-1}$. These examples underscore that specific functional groups, such as hydroxyl, and oxygen-containing groups, as well as composite structures such as the ones found in chitosan composites, can dramatically enhance adsorption capacities, sometimes even more than materials with larger surface areas but without such chemical modifications.

Conversely, materials like carbon black from recycled tires, with an S_{BET} of 57 $m^2 \cdot g^{-1}$, show much lower adsorption capacities (0.54 $mg \cdot g^{-1}$ for Nd). This indicates that without functionalization, grafting, or intrinsic mineral content, materials with lower surface areas tend to have reduced adsorption capabilities [33]. Comparatively, chars from spent-tire rubber with similar low surface areas (74 $m^2 \cdot g^{-1}$) exhibit higher adsorption capacities (32.8 $mg \cdot g^{-1}$ for Nd) due to the presence of metals in their matrix [14] that can participate in an ion-exchange mechanism. Similarly, the ordered mesoporous carbon (CMK-8) shows a significant increase in adsorption capacity when oxidized (22.3 $mg \cdot g^{-1}$) compared to its non-oxidized form (3.31 $mg \cdot g^{-1}$), despite a minor increase in surface area (from 914 $m^2 \cdot g^{-1}$ to 933 $m^2 \cdot g^{-1}$) [23].

In summary, while surface area is a critical factor in determining the adsorption capacity of carbon-based materials for the adsorption of REEs, the presence of functional groups, grafted compounds, or mineral content often plays a more pivotal role in the adsorption mechanisms. Materials with lower surface areas but significant functionalization or grafting

can outperform those materials with higher surface areas but no modifications, highlighting the importance of chemical modifications in enhancing adsorption performance.

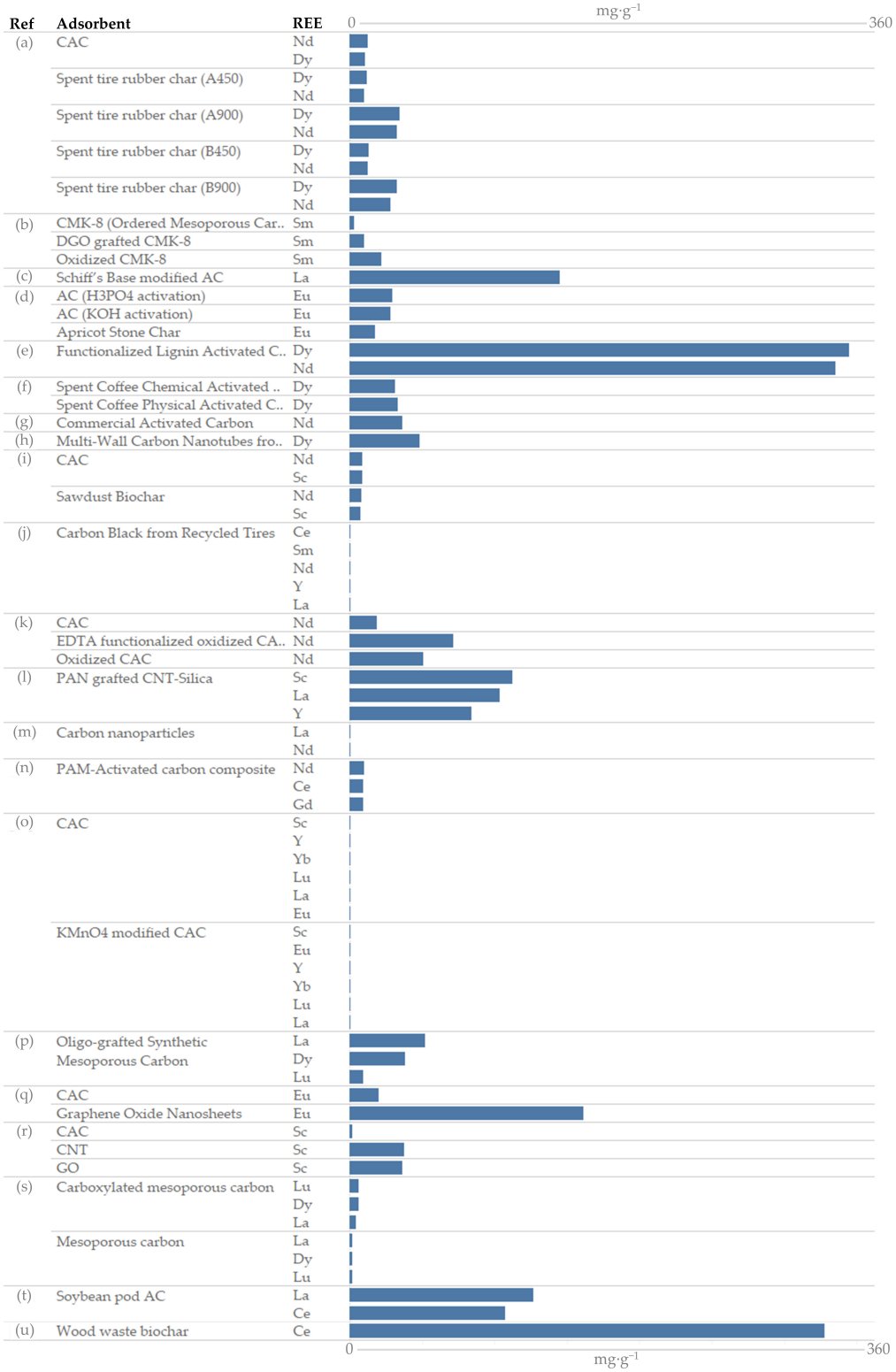

Figure 2. Maximum adsorption capacity of all the reviewed adsorbents; References: (a)—[14]; (b)—[23]; (c)—[24]; (d)—[25]; (e)—[28]; (f)—[29]; (g)—[30]; (h)—[31]; (i)—[32]; (j)—[33]; (k)—[34]; (l)—[36]; (m)—[38]; (n)—[39]: (o)—[40]; (p)—[41]; (q)—[42]; r—[43]; (s)—[44]; (t)—[45]; (u)—[46].

3. Adsorption Mechanisms and Influencing Factors

The adsorption of REEs onto carbon-based materials involves several mechanisms (Figure 3), each contributing to the overall adsorption capacity and efficiency [8,26,47]. Understanding these mechanisms is crucial for optimizing the design and application of adsorbents. The primary adsorption mechanisms include the following:

i. Physical adsorption: Physical adsorption, also known as physisorption, is driven by van der Waals forces and other weak bonds. It occurs when REE ions are attracted to the surface of the carbon-based adsorbent without any chemical bonding. This type of adsorption is usually reversible and depends on the surface area and pore structure of the adsorbent [6,8].

ii. Electrostatic interactions: Electrostatic interactions involve the formation of strong chemical bonds between REE ions and the functional groups on the surface of the carbon material. This process is usually irreversible and results in a stronger attachment of the REEs to the adsorbent. Functional groups such as carboxyl, hydroxyl, and phenolic groups play a crucial role in electrostatic interactions, enhancing the adsorption capacity by providing specific binding sites for REEs [28,29,41].

iii. Ion exchange: Ion exchange is a process where REE ions in solution replace other ions on the surface of the adsorbent. This mechanism is highly dependent on the pH of the solution and the presence of ionizable functional groups on the adsorbent. Ion exchange is particularly effective in materials such as modified activated carbons, chars, and biochars that have been functionalized to enhance their ion-exchange capacities or are rich in mineral content that can perform ionic exchange [14,34,35].

iv. Complexation: Complexation involves the formation of coordination complexes between REE ions and functional groups on the adsorbent surface. This mechanism is influenced by the type and availability of functional groups, such as amino, carboxyl, and phosphonic groups. Complexation often leads to the formation of stable REE–ligand complexes, significantly enhancing the adsorption capacity of the material [28,29,34].

v. Precipitation: Precipitation occurs when REE ions react with functional groups or counter-ions present on the adsorbent surface, leading to the formation of insoluble REE compounds that deposit onto the adsorbent. This mechanism is typically influenced by factors such as pH, ion concentration, and the presence of specific anions, which can form insoluble REE salts. Precipitation can enhance the overall adsorption efficiency by reducing the concentration of REE ions in solution, particularly under conditions that favor the formation of stable precipitates [48,49].

Several factors affect the efficiency of REE adsorption onto carbon-based materials. These factors include the following:

i. Surface area: The surface area of the adsorbent is a critical factor influencing adsorption capacity. Materials with higher surface areas usually provide more adsorption sites, leading to greater adsorption capacities [38,42].

ii. Pore size distribution: The pore size distribution of the adsorbent affects the accessibility of REE ions to the adsorption sites. Micropores (pores < 2 nm) contribute to high adsorption capacities by providing a large surface area, while mesopores (2–50 nm) and macropores (>50 nm) facilitate the diffusion of REE ions into the interior of the adsorbent. Optimal pore size distribution ensures efficient utilization of the adsorbent's surface area [32,33].

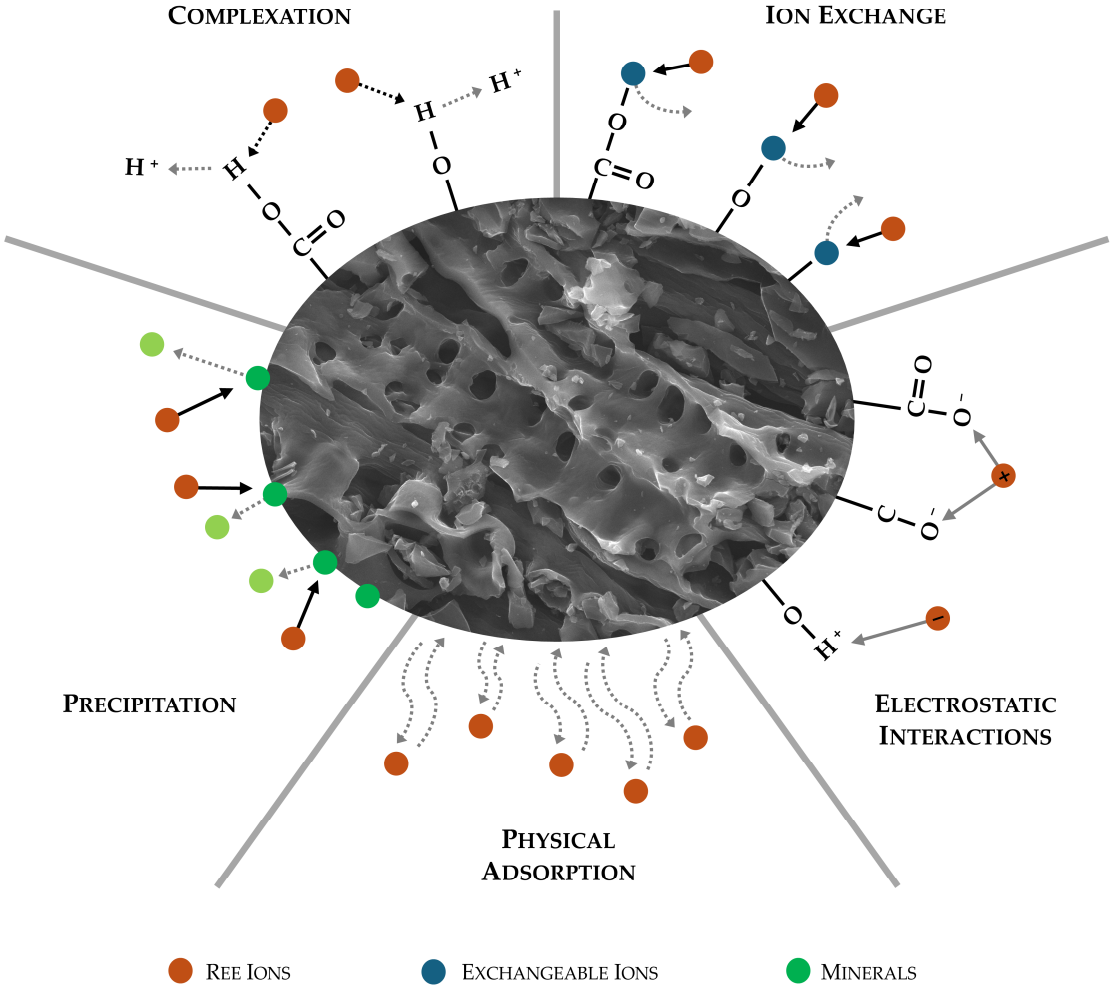

Figure 3. Schematic of the main adsorption mechanisms of REEs onto pyrolytic carbon-based adsorbents; Arrows represent the interactions between the adsorbent and REE ions; adapted from [48,50].

iii. Functional groups: The presence and type of functional groups on the surface of the adsorbent materials characterize the chemical nature of the surface and are crucial for their adsorption capacity. Functional groups such as carboxyl, hydroxyl, and amino groups enhance adsorption capacity through chemisorption, ion exchange, and complexation mechanisms. Recent studies have demonstrated that surface functionalization of carbon materials can significantly improve adsorption performance by introducing or increasing these functional groups [48,49,51]. Modifications such as the addition of oxygen-containing groups (e.g., carboxyl and hydroxyl), nitrogen-containing groups (e.g., amine and imine), and phosphorus-containing groups (e.g., phosphonate) have been shown to enhance adsorption by providing more active and selective binding sites for REEs [34,36]. Carboxyl (-COOH) groups enhance ion exchange and complexation by ionizing in aqueous solutions, particularly at neutral-to-alkaline pH. The resulting R-COO^- attracts REE ions via electrostatic interactions and can form coordination bonds that can improve adsorption capacities. Hydroxyl (-OH) groups contribute to adsorption by forming hydrogen bonds and deprotonating in alkaline conditions, allowing strong interactions with REE ions. They boost the adsorption of metal ions by facilitating surface complex formation and increasing adsorbent hydrophilicity. Nitrogen-containing groups such as amino (-NH_2) and imine (-C=NH) groups enhance adsorption through coordination bonds, where nitrogen donates electrons to form stable complexes with REEs. Phosphonate (-PO_3H_2) groups offer multiple binding sites, forming stable chelate complexes with

metal ions. Other functional groups, such as carbonyl (-C=O) and ether (-C-O) groups, also enhance metal adsorption by forming surface complexes. The functionalization of carbon materials with these groups not only increases the adsorption capacity but also improves selectivity in the presence of competing metal ions. Molecular-level studies indicate that these modifications enhance the coordination environment for REEs, leading to stronger and more stable adsorption. Furthermore, advanced surface modifications, such as grafting ligands or chelating agents onto carbon-based adsorbents, can further boost adsorption efficiency by creating highly selective binding sites for REEs.

iv. pH: The pH of the solution influences the ionization state of both the REE ions and the functional groups on the adsorbent. At low pH, hydrogen ions compete with REE ions for adsorption sites, reducing adsorption efficiency. Conversely, at higher pH values, the functional groups are more ionized, enhancing their ability to bind REE ions. Optimal pH conditions must be determined for each adsorbent–REE system to maximize adsorption efficiency [37,40].

v. Temperature: Temperature affects the kinetics and equilibrium of the adsorption process. Higher temperatures typically increase the diffusion rate of REE ions into the pores of the adsorbent, potentially enhancing the adsorption capacity, particularly for endothermic adsorption processes where heat absorption facilitates ion interaction and binding [52]. However, extreme temperatures can also disrupt the stability of adsorbent-REE interactions, particularly in chemisorption and complexation processes [42,43]. Conversely, in exothermic adsorption processes, where heat is released, higher temperatures can disrupt the stability of adsorbent-REE interactions and decrease adsorption capacity [53]. Therefore, the effect of temperature on adsorption efficiency depends on whether the adsorption process is exothermic or endothermic, with each mechanism exhibiting distinct behaviors under varying thermal conditions.

vi. Presence of competing ions: The presence of other ions in solution can compete with REE ions for adsorption sites, affecting the selectivity and capacity of the adsorbent. For example, the presence of common metal ions like calcium and magnesium can reduce the adsorption efficiency of REEs. Understanding the competitive adsorption behavior is essential for developing selective adsorbents for REE recovery from complex matrices [14,25,40].

By optimizing these factors, the adsorption efficiency of carbon-based materials for REEs can be significantly enhanced, contributing to more effective and sustainable recovery processes.

4. Batch versus Dynamic Adsorption Assays

Batch adsorption assays are based on mixing a known mass of adsorbent with a solution containing specific concentrations of adsorbate. The mixture is then agitated for a determined time, allowing the adsorbate to interact with the adsorbent until the adsorption equilibrium is reached. Afterward, the adsorbate concentration remaining in the solution is quantified, and the adsorption capacities of the materials are determined this way [54–57]. A majority of the studies on the adsorption of REEs onto carbon-based materials are performed in batch conditions, as evidenced by Table 2.

The benefits of applying batch conditions to these assays are as follows:

i. Simplicity and convenience: These assays are very straightforward to perform, requiring only basic equipment, such as a vessel to hold the mixture, a means to agitate or shake the mixture, and a system to separate the adsorbent from the mixture after the equilibrium is reached (filtration or centrifugation).

ii. Controlled conditions: The factors that control the adsorption processes, such as pH, temperature, and initial adsorbate concentrations, can be easily controlled and adjusted, facilitating the comprehension of their effects on the adsorption processes.

iii. Basic kinetic and isotherm data: This type of adsorption assay allows users to obtain basic kinetic and isotherm data that provide a fundamental understanding of the adsorption process.
iv. Cost-effectiveness: The batch mode is relatively inexpensive when compared to dynamic assays, as it requires less equipment, as well as lower quantities of adsorbent and adsorbate.

Nevertheless, batch adsorption studies also suffer from some limitations, such as the following:

i. Equilibrium limitations: Batch assays assume equilibrium conditions, which may not correctly reflect the dynamic nature of the adsorption process under industrial-scale processes.
ii. Limited information: They provide limited information on the complex dynamics of the adsorption processes over time. For example, diffusional constraints cannot be assessed through batch assays.
iii. Scale-up challenges: The results obtained from batch assays rarely correlate to large-scale and/or industrial processes, thus hindering the upscaling of the application of these materials into real-stream scenarios. Only in very limited situations, the industrial processes are running in completely mixed systems, as occurs in batch adsorption assays.

On the other hand, dynamic adsorption assays, also known as column assays, rely on circulating the adsorbate solution through a column filled with adsorbent materials [58]. The effluent is then collected at the output of the column, over time, and the adsorbate concentration is then quantified to determine the adsorption capacities and kinetics [54–56,59]. The available literature in which dynamic assays were performed is very scarce concerning REEs' adsorption, with only one study in this review being conducted in this manner, as can be seen in Table 2.

The major advantages of dynamic assays are as follows:

i. Realistic conditions: Column assays simulate continuous flow conditions, which provide a more realistic representation of industrial processes while providing better insights into real-world applications.
ii. Kinetic information: These dynamic studies offer detailed information on adsorption kinetics, breakthrough performances, and mass transfer characteristics.
iii. Scalability: Contrary to batch studies, dynamic assays have a higher correlation with industrial processes, facilitating the scale-up and design of large-scale adsorption systems.

The limitations of the application of dynamic adsorption assays are as follows:

i. Complexity: This type of adsorption assay requires more sophisticated equipment, such as columns, pumps, piping, and collectors, resulting in more complex setups that are harder to implement.
ii. Higher costs: Following the previous point, these more complex systems are more expensive and incur higher operating costs due to the need for continuous operation and larger quantities of adsorbates.
iii. Operational challenges: With higher complexity comes more opportunities for operation problems to appear and hinder the success of these assays. Factors such as column clogging, channeling, development of preferable pathways, and pressure drops can affect the performance and accuracy of dynamic assays.

Both batch and dynamic adsorption assays have their distinct advantages and limitations [55]. Batch assays are ideal for preliminary studies and understanding basic adsorption characteristics under controlled conditions. In contrast, dynamic assays are essential for investigating the practical applicability of adsorbents in continuous systems, providing insights into adsorption kinetics and scalability. For the adsorption of REEs onto carbon-based materials, employing both batch and dynamic assays can offer a comprehensive understanding of the involved processes. Initial batch studies can identify promising

adsorbents and optimal conditions, while dynamic assays can validate these findings under continuous flow conditions, simulating real-world applications.

Incorporating both batch and dynamic adsorption assays in research provides a more suitable approach to evaluating the performance of carbon-based adsorbents for REE recovery. Future studies should aim to bridge the gap between laboratory-scale experiments and real-world applications, ensuring the development of economically and environmentally sustainable adsorption processes.

5. Adsorption Isotherms, Kinetic, and Breakthrough Models

The articles reviewed employ various adsorption isotherm and kinetic models to describe and analyze the adsorption behavior of REEs onto carbon-based materials. As stated in the previous section, most studies only performed batch assays, resulting in only batch models being applied. The most used models include the Langmuir and Freundlich isotherm models [60–63], as well as pseudo-first-order and pseudo-second-order kinetic models [24,63–66]. These models contributed to the understanding of adsorption mechanisms and the efficiency of different adsorbents.

5.1. Batch Isotherm Models

The Langmuir isotherm model assumes monolayer adsorption onto a surface with a finite number of identical sites [61–63,67]. It is described by Equation (1):

$$q_e = \frac{q_m \cdot K_L \cdot C_e}{1 + K_L \cdot C_e} \quad (1)$$

where q_e is the amount of adsorbate adsorbed per unit mass of adsorbent ($mg \cdot g^{-1}$), q_m is the maximum adsorption capacity ($mg \cdot g^{-1}$), K_L is the Langmuir constant related to the affinity of binding sites ($L \cdot mg^{-1}$), and C_e is the equilibrium concentration of adsorbate ($mg \cdot L^{-1}$).

The Freundlich isotherm model, on the other hand, is an empirical model that assumes adsorption on heterogeneous surfaces [61–63,68]. It is described by Equation (2):

$$q_e = K_F \cdot C_e^{1/n} \quad (2)$$

where K_F ($mg \cdot g^{-1}$)($mg \cdot L^{-1}$)^n and n (dimensionless) are the Freundlich constants indicative of adsorption capacity and adsorption intensity, respectively; and C_e is the equilibrium concentration of adsorbate ($mg \cdot L^{-1}$).

More advanced and mechanistic batch isotherm models also exist, such as the Sips isotherm model, however, no study presented in this review applied it. The Sips isotherm model is a hybrid model that combines the Langmuir and Freundlich isotherms, useful for predicting heterogeneous adsorption systems at high adsorbate concentrations [69]. It is described by Equation (3):

$$q_e = \frac{q_m \cdot (K_S \cdot C_e)^{1/n}}{1 + (K_S \cdot C_e)^{1/n}} \quad (3)$$

where q_m is the maximum adsorption capacity ($mg \cdot g^{-1}$), C_e is the equilibrium concentration of adsorbate ($mg \cdot L^{-1}$), K_S ($mg \cdot L^{-1}$) is the Sips constant, and n (dimensionless) is the heterogeneity factor.

5.2. Batch Kinetic Models

The pseudo-first-order kinetic model is based on the assumption that the rate of occupation of adsorption sites is proportional to the number of unoccupied sites [63–66,70]. It is represented by Equation (4):

$$q_t = q_e \cdot \left[1 - e^{-k_f \cdot t}\right] \quad (4)$$

where q_t is the amount of adsorbate adsorbed at time t (mg·g^{-1}), q_e is the amount of adsorbate adsorbed at equilibrium (mg·g^{-1}), and k_f is the rate constant of the pseudo-first-order adsorption (min^{-1}).

The pseudo-second-order kinetic model assumes that the rate of adsorption is proportional to the square of the number of unoccupied sites [64–66,71]. It is described by Equation (5):

$$q_t = \frac{k_s \cdot q_e^2 \cdot t}{1 + q_e \cdot k_s \cdot t} \quad (5)$$

where k_s is the rate constant of the pseudo-second-order adsorption (g·mg^{-1}·min^{-1}).

The Elovich, the Weber–Morris intra-particle diffusion, and the Avrami kinetic models offer additional advanced ways to model the experimental data obtained from the adsorption assays, but they were not applied in the studies presented in this review. The Elovich kinetic model describes the kinetics of chemisorption processes, particularly for systems with heterogeneous surfaces [72,73]. It is described by Equation (6):

$$\frac{dq_t}{dt} = \alpha \cdot e(-\beta q_t) \quad (6)$$

where q_t is the amount of adsorbate adsorbed at time t (mg·g^{-1}), and α (mg·g^{-1}·min^{-1}) and β (g·mg^{-1}) are constants.

The Weber–Morris intra-particle diffusion model is used to identify the rate-controlling steps in the adsorption process by considering intra-particle diffusion [74,75]. It is described by Equation (7):

$$q_t = k_{id} \cdot t^{0.5} + C \quad (7)$$

where q_t is the amount of adsorbate adsorbed at time t (mg·g^{-1}), k_{id} (mg·g^{-1}·min$^{-0.5}$) is the intra-particle diffusion rate constant, and C (mg·g^{-1}) is the intercept, which represents the boundary layer effect.

The Avrami kinetic model describes the kinetics of phase change processes and can be adapted for adsorption kinetics [76]. It is described by Equation (8):

$$q_t = q_{\mathrm{m}} \cdot (1 - e(-k_A \cdot t^n)) \quad (8)$$

where q_t is the amount of adsorbate adsorbed at time t (mg·g^{-1}), q_m is the maximum adsorption capacity (mg·g^{-1}), k_A (min^{-n}) is the Avrami rate constant, and n is the Avrami exponent.

5.3. Breakthrough Models

Dynamic adsorption studies normally revolve around column assays and use different models to describe the breakthrough curves and the mass transfer processes. The most commonly used models are the Thomas model, the Yoon–Nelson model, and the Bohart–Adams model. The Thomas model assumes plug flow behavior in the column and uses pseudo-first-order reaction kinetics to describe the adsorption process [55,77,78]. It is described by Equation (9):

$$\ln\left(\frac{C_0}{C_t} - 1\right) = k_{Th} \cdot q_0 \cdot W - k_{Th} \cdot C_0 \cdot t \quad (9)$$

where C_0 is the influent adsorbate concentration (mg·L^{-1}), C_t is the effluent adsorbate concentration (mg·L^{-1}) at time t, k_A is the Thomas rate constant (L·mg^{-1}·min^{-1}), k_A is the maximum solid-phase concentration (mg·g^{-1}), and W is the mass of adsorbent (g).

The Yoon–Nelson model simplifies the adsorption process by assuming that the probability of adsorbate breakthrough is proportional to the adsorbed amount [59,79,80]. It is described by Equation (10):

$$\ln\left(\frac{C_t}{C_0 - C_t}\right) = k_{YN} \cdot t - \tau \quad (10)$$

where C_0 is the influent adsorbate concentration (mg·L^{-1}), C_t is the effluent adsorbate concentration (mg·L^{-1}) at time t, k_{YN} is the rate constant (min^{-1}), and τ is the time required for breakthrough (min).

The Bohart–Adams model assumes that adsorption is controlled by the surface reaction between the adsorbate and adsorbent [59,81,82]. It is described by Equation (11):

$$\ln\left(\frac{C_t}{C_0}\right) = k_{BA}\cdot C_0\cdot t - k_{BA}\cdot N_0\cdot Z \quad (11)$$

where C_t is the effluent adsorbate concentration (mg·L^{-1}) at time t, C_0 is the influent adsorbate concentration (mg·L^{-1}), k_{BA} is the rate constant (L·mg^{-1}·min^{-1}), N_0 is the adsorption capacity per unit of volume (mg·L^{-1}), and Z is the bed depth (cm).

5.4. Model Comparisons and Data Fitting

Table 3 presents the isotherm and kinetic model data that better fit the experimental data from the works studied in this review.

Table 3. Kinetic and isotherm model data; PFO, pseudo-first order; PSO, pseudo-second order; IDM, intra-particle diffusion model.

Adsorbent	Tested REE	Isotherm Model	Isotherm Constant Value		Kinetic Model	Kinetic Constant Value		Ref.
Functionalized lignin-activated carbon	Nd	-	-		PSO	1.14×10^{-4}	g·mg^{-1}·min^{-1}	[28]
					IDM	24	mg·g^{-1}·min$^{-1/2}$	
Functionalized lignin-activated carbon	Dy				PSO	3.39×10^{-4}	g·mg^{-1}·min^{-1}	
Spent coffee physical-activated carbon	Dy	Langmuir	6.42	L·mg^{-1}	PSO	1.017	$\times 10^{-3}$	[29]
Spent coffee chemical-activated carbon			10.50			1.232		
Commercial activated carbon	Nd	Langmuir	3.49	L·g^{-3}	PFO	0.138	min^{-1}	[30]
Multi-wall carbon nanotubes from crystalline nanocellulose	Dy	Langmuir	0.64	L·g^{-3}	PSO	0.093	g·mg^{-1}·min^{-1}	[31]
Sawdust biochar	Nd	Freundlich	-		PSO	0.875	g·mg^{-1}·min^{-1}	[32]
	Sc					2.723		
Commercial activated carbon (CAC)	Nd					2.258		
	Sc					13.79		
Carbon black from recycled tires	Nd	Langmuir	18.8	L·mol^{-1}	PSO	0.136	g·mg^{-1}·min^{-1}	[33]
	La		51.4			0.111		
	Ce		30.2			0.516		
	Sm		19.3			0.098		
	Y		6.1			0.107		
Commercial activated carbon (CAC)	Nd	Langmuir	-	L·mg^{-1}	PSO	-	g·mg^{-1}·min^{-1}	[34]
Oxidized CAC			-			-		
EDTA-functionalized oxidized CAC			0.130			0.042		
Oxidized carbon nanofibers	La	-	-		-	-		[35]
	Eu							
	Gd							
	Yb							
PAN-grafted carbon nanotubes–silica	La	Langmuir	-		PSO	-		[36]
	Sc							
	Y							
Carbon xerogel–chitosan composite	-	Freundlich	25.2	L·mg^{-1}	PSO	1.35×10^{-4}	min^{-1}	[37]
Carbon nanoparticles	Nd	-	-		-	-		[38]
	La							
PAM-activated carbon composite	Nd	-	-		PSO	0.312	g·mg^{-1}·min^{-1}	[39]
	Ce					0.315		
	Gd					0.147		

Table 3. *Cont.*

Adsorbent	Tested REE	Isotherm Model	Isotherm Constant Value		Kinetic Model	Kinetic Constant Value		Ref.
Commercial activated carbon	La	Langmuir	0.291	$L \cdot \mu g^{-1}$	PSO	0.776	$10^{-2} \cdot g \cdot \mu g^{-1} \cdot min^{-1}$	[40]
	Yb		0.250			0.126		
	Lu		0.257			0.236		
	Eu		0.378			0.378		
	Y		0.182			0.471		
	Sc		0.330			0.942		
$KMnO_4$-modified commercial activated carbon	La		1.110			1.560		
	Yb		0.612			1.800		
	Lu		1.780			1.990		
	Eu		1.760			2.410		
	Y		0.601			1.630		
	Sc		1.220			1.900		
Oligo-grafted synthetic mesoporous carbon	Lu Dy La	-	-		-	-		[41]
Commercial activated carbon	Eu	Langmuir	0.398	$L \cdot mg^{-1}$	-	-		[42]
Graphene oxide Nanosheets			0.185					
Commercial activated carbon	Sc	-	-		IDM	0.32	$10^{-2} \cdot g \cdot mg^{-1} \cdot min^{-1}$	[43]
Carbon nanotubes						0.27		
Graphite oxide						0.22		
Apricot stone char	Eu	Langmuir	-	$L \cdot mg^{-1}$	-	-	$g \cdot mg^{-1} \cdot min^{-1}$	[25]
Activated carbon (H_3PO_4 activation)			0.034		PSO	0.034		
Activated carbon (KOH activation)			-		-	-		
Schiff's base-modified activated carbon	La	Langmuir	0.1	$L \cdot mg^{-1}$	PSO	0.004	$g \cdot mg^{-1} \cdot min^{-1}$	[24]
CMK-8 (ordered mesoporous carbon)	Sm	Langmuir	0.480	$L \cdot mg^{-1}$	PSO	368.25	$g \cdot mg^{-1} \cdot min^{-1}$	[23]
Oxidized CMK-8			0.080			2.89		
DGO-grafted CMK-8			0.660			9.26		
Spent tire-rubber char (A450)	Nd	Langmuir	0.937	$L \cdot mg^{-1}$	PSO	0.003	$g \cdot mg^{-1} \cdot min^{-1}$	[14]
	Dy		0.147			0.032		
Spent tire-rubber char (B450)	Nd		0.948			0.006		
	Dy		0.232			0.013		
Spent tire-rubber char (A900)	Nd		0.763			0.073		
	Dy		0.656			0.049		
Spent tire-rubber char (B900)	Nd		0.254			0.020		
	Dy		0.317			0.022		
Commercial activated carbon	Nd		0.155			1.070		
	Dy		0.256			0.758		
Mesoporous carbon	La Dy Lu	-	-		-	-		[44]
Carboxylated mesoporous carbon	La Dy Lu							
Soybean pod-activated carbon	Ce	Langmuir	0.224	$L \cdot mg^{-1}$	PSO	0.006	$g \cdot mg^{-1} \cdot min^{-1}$	[45]
	La		0.226			0.005		
Wood-waste biochar	Ce	Langmuir	0.660	$L \cdot mg^{-1}$	PFO	0.037	min^{-1}	[46]

Many studies, such as those by Alcaraz et al. [29], found that the Langmuir isotherm model provided a better fit to their experimental data, suggesting monolayer adsorption on a homogeneous surface. For instance, Alcaraz et al. [29] reported high correlation coefficients (R^2) for the Langmuir model, indicating that spent coffee-activated carbons absorb REEs in a monolayer fashion. This fit reflects the high adsorption capacities observed for Dy (33.52 and 31.26 $mg \cdot g^{-1}$).

Conversely, some studies, such as those by Komnitsas et al. [32], using sawdust biochar, found that the Freundlich isotherm model better described their adsorption data, indicating adsorption on a heterogeneous surface with varying affinities. This model fit correlates with the lower adsorption capacities (8.0 $mg \cdot g^{-1}$ for Nd and 7.5 $mg \cdot g^{-1}$ for Sc), as it reflects a more diverse range of adsorption sites with differing strengths.

Regarding kinetic models, the pseudo-second-order model generally provided a better fit for the adsorption processes studied, as seen in Table 3. The superior fit of this model suggests that chemisorption, involving valence forces through the sharing or exchange of electrons between adsorbent and adsorbate, is the rate-limiting step. For example, the high adsorption capacities of 33.5 $mg \cdot g^{-1}$ for Nd and 344.6 $mg \cdot g^{-1}$ for Dy on functionalized lignin-activated carbon [28] align well with the pseudo-second-order model, reflecting the strong chemical interactions between the adsorbate and the functionalized adsorbent.

Concerning breakthrough models applied to the adsorption of REEs onto carbon-based materials, no data are available, as the only dynamic study present in this review, the one performed by Chen et al. [35], did not model the experimental data they obtained in the performed assays.

The fitting of these models to the experimental data is crucial for understanding the adsorption mechanisms and predicting adsorption performance. Materials that align well with the Langmuir model, such as functionalized lignin-activated carbon and phosphorus-functionalized nanoporous carbon, tend to exhibit high adsorption capacities due to the uniform and high-affinity binding sites. In contrast, materials described by the Freundlich model, like sawdust biochar, demonstrate lower capacities, indicating more variable site affinities and less efficient adsorption.

The use of the pseudo-second-order kinetic model in many studies highlights the importance of chemical interaction in achieving high adsorption capacities. Adsorbents that exhibit strong chemical interactions with REEs, facilitated by functional groups, grafting, or mineral content, tend to show higher adsorption capacities and better fit this kinetic model.

Understanding the models used in batch and dynamic adsorption studies is crucial for interpreting experimental data and optimizing adsorption processes [61,83]. Batch models, like Langmuir and Freundlich, and advanced models, such as Sips, Elovich, Weber–Morris, and Avrami, provide insights into the adsorption capacity and surface characteristics of adsorbents. Kinetic models help in understanding the rate-controlling steps of the adsorption process. Dynamic models, on the other hand, are essential for designing and scaling up adsorption systems for real-world applications. Models like Thomas, Yoon–Nelson, and Bohart–Adams provide valuable information on the breakthrough behavior and mass transfer processes in fixed-bed columns.

Incorporating both batch and dynamic models in research allows for a comprehensive evaluation of carbon-based adsorbents for REEs' recovery. This approach not only helps in identifying the best adsorbents under controlled conditions but also validates their performance in continuous flow systems, paving the way for practical and scalable adsorption processes. By integrating these models, researchers can develop more efficient and economically viable methods for the recovery of REEs.

6. Post-Adsorption Processes for Rare Earth Elements on Carbon-Based Materials

Following the adsorption of REEs onto carbon-based materials, the most common pathway is desorption assays, which are used to assess the efficiency and feasibility of the recovery process.

Desorption involves the removal of the adsorbed REEs from the carbon materials, typically achieved through chemical treatments or changes in solution conditions, such as the pH, ionic strength, or temperature [27,84].

For instance, Gad and Awwad conducted desorption studies on Eu using AC, demonstrating that the desorption efficiency is significantly influenced by the choice of desorbing agent and the operational parameters, such as the pH and contact time [25]. Similarly, Babu et al. studied the desorption of REEs on EDTA-functionalized ACs to desorb REEs using HCl solutions (0.01 M to 1 M), showcasing the potential for multiple adsorption-desorption cycles without significant loss in capacity [34].

Also, Marwani et al. studied the desorption of La using HCl solutions, reporting that higher HCl concentrations would improve the amount of REE desorbed from the carbon materials [24]. Perreault et al. evaluated the efficiency of REE desorption using

oxalate solutions ($(NH_4)_2C_2O_4$) and found that this method was able to desorb around 80% of the REEs from the carbon material, and after five cycles, the adsorption efficiency decreased by 10% [23]. Haggag et al. investigated seven different chemical compounds (HCl, H_2SO_4, HNO_3, Na_2CO_3, NaCl, Na_2SO_4, and CH_3COONa) for REEs' desorption, and their results showed that HCl was the best desorption agent, with a REE desorption efficiency of 98.2% [37].

Another pathway for the utilization of carbon-based materials loaded with REEs, at the post-adsorption, is the repurposing of these materials as catalysts for various chemical reactions [85,86]. The unique properties of REEs, such as their redox behavior and ability to stabilize high oxidation states, make them excellent candidates for catalytic processes [85,86]. For example, Gong et al. studied a REE-loaded AC as a catalyst for the selective catalytic reduction of NO with NH_3, leveraging the catalytic capabilities of REEs to enhance reaction rates and efficiencies [87]. El-Khouly et al. also studied the photocatalytic properties of a REE-loaded AC. This study focused on Ce-loaded peach stone AC as a catalyst for the photodegradation of Maxilon Red dye. The authors reported that the REE-loaded AC improved the catalytic performance owing to its wide band-gap energy and redox reactions [88]. Chu et al. reported that REE-loaded carbon black was an efficient electrocatalyst for oxygen reduction reactions in proton-exchange membrane fuel cells due to their high stability and activity [89].

Carbon materials loaded with REEs can also be utilized in environmental remediation [90]. These materials can serve as adsorbents for further purification of water and air, capturing additional contaminants through a synergistic adsorption process. The REE-loaded carbon materials, such as those investigated by Yu et al., where a Ce-loaded AC was studied for the removal of arsenate and arsenite from wastewaters, suggest that these materials have the potential to be applied for water decontamination [91].

In summary, after the adsorption of REEs onto carbon-based materials, several post-adsorption processes, such as desorption assays, catalytic applications, environmental remediation, and regeneration, are employed to maximize the utility and sustainability of the materials. These processes not only enhance the recovery of valuable REEs but also extend the functional lifespan of the carbon-based adsorbents.

7. Future Directions: Synthetic Solutions versus Real Leachates

Most studies investigating the adsorption of REEs onto carbon-based materials have utilized synthetic solutions, as evidenced by this review, where controlled concentrations of individual REEs or mono-component solutions are prepared in the laboratory. These synthetic solutions provide a simplified and controlled environment that allows researchers to isolate and examine the adsorption capacities, kinetics, and isotherm models of specific adsorbents without interference from other compounds. For example, Saha et al. [41], Alcaraz et al. [29], and Nogueira et al. [14] conducted their experiments using synthetic solutions of Nd and Dy, which helped precisely determine the adsorption capacities of the functionalized lignin-activated carbon, spent coffee-activated carbon, and spent-tire chars, respectively.

While synthetic solutions are valuable for fundamental research, they do not fully replicate the complexities of real-world scenarios [6,9,92]. In practical applications, REEs are typically found in mixed-waste streams, such as industrial effluents, mining leachates, and electronic-waste leachates, which contain a variety of other metals, organic compounds, and competing ions [9,92]. These additional components can significantly influence the adsorption behavior and efficiency of the adsorbents [14].

To bridge the gap between laboratory research and real-world applications, future studies should focus on evaluating the performance of pyrolytic carbon-based adsorbents using real leachates or mixed solutions containing REEs. Real leachates present a more challenging and realistic environment, where multiple factors, such as pH variations, the presence of competing ions, and organic matter, can affect the adsorption process.

Understanding how these factors impact the adsorption capacities and mechanisms will be crucial for developing effective and scalable technologies for REE recovery.

For instance, real leachates from electronic waste or mining operations typically contain a complex mixture of metals and other contaminants [6,7,12,92]. Adsorbents that perform well in synthetic solutions might exhibit reduced efficiency or selectivity in such environments. Therefore, it is essential to test these materials in conditions that closely mimic actual waste streams to evaluate their true potential and identify any necessary modifications or enhancements.

Conducting adsorption studies using real leachates will also provide insights into the regeneration and reuse of adsorbents, a critical factor for the economic viability of REE recovery processes. Adsorbents need to maintain high adsorption capacities over multiple cycles of adsorption and desorption in the presence of complex mixtures. Research in this area will help in optimizing the operational parameters and improving the sustainability of the adsorption processes.

The most recent studies on the adsorption of REEs by Saha et al. (2023), Pinheiro et al. (2023), and Reis et al. (2023) applied the produced carbon-based materials in real leachates, underscoring that the application in real leachates is important and indeed a needed process in these types of studies. Saha et al. studied the recovery of REEs from coal fly ash leachates (HNO_3 leaching) using a carboxylated mesoporous carbon, achieving 80–90% recovery of sixteen REEs from the coal fly ash leachates, although the REE concentration in the leachates was in the ppb range [44]. Pinheiro et al. used soybean pod AC for the recovery of Ce and La from real phosphogypsum leachate, a waste by-product of phosphate fertilizer or phosphoric acid production. They were able to achieve adsorption capacities of 67.6 and 33.7 $mg \cdot g^{-1}$ for Ce and La, respectively, on the real leachates [45]. Reis et al. also applied their produced biochar for the recovery of REEs from phosphogypsum leachate, with their wood-waste biochar being able to recover 86% of the Ce present in the leachate [46].

In conclusion, while studies using synthetic solutions have provided valuable foundational knowledge, the next step is to focus on real leachates to ensure that the developed adsorption technologies are robust, efficient, and applicable to real-world scenarios. This focus will help in advancing the field toward practical and scalable solutions for the sustainable recovery of REEs from various waste streams.

8. Challenges and Gaps in Current Research

Despite the promising attributes of pyrolytic carbon-based materials for REEs' adsorption, several challenges and gaps remain in current research. One of the primary challenges is the variability in adsorption performance due to differences in the physicochemical properties of the adsorbents. Factors such as surface area, pore size distribution, and the nature and density of functional groups can vary significantly depending on the source material and production methods. This variability complicates the comparison of results across different studies and makes it difficult to identify the most effective adsorbent materials and optimal production conditions [8,26].

Another significant gap is the limited understanding of the adsorption mechanisms at a molecular level [14,26,93]. While it is known that various functional groups on carbon-based materials interact with REE ions, the precise nature of these interactions and the relative contributions of different mechanisms are not fully elucidated. Advanced analytical techniques and theoretical modeling studies are needed to provide deeper insights into these mechanisms and to guide the design of more effective adsorbents [8].

Moreover, most studies on REE adsorption using carbon-based materials have been conducted under controlled laboratory conditions with synthetic solutions [26]. These conditions often do not accurately reflect the complexity of real-world scenarios, where REEs are present in mixtures with other metals and organic compounds, and where pH, temperature, and ionic strength can vary widely. Consequently, there is a scarcity of research involving real e-waste leachates or industrial effluents, thus limiting the practical applicability of the findings. Addressing this gap requires more field studies and pilot-scale

experiments to validate the performance of pyrolytic carbon-based adsorbents in diverse and realistic environments for REEs' adsorption.

In addition to these challenges, emerging technologies and interdisciplinary approaches offer promising avenues to address some of the identified gaps. Machine learning (ML) and artificial intelligence (AI) models, for instance, have the potential to predict adsorption behaviors based on adsorbent characteristics, optimizing the selection of pyrolytic carbon-based materials for specific REE recovery applications [94–96]. By integrating large datasets from experimental studies, ML models can identify patterns and predict outcomes that would otherwise require extensive trial-and-error experimentation. Furthermore, the development of nano-engineered adsorbents, which leverage nanoscale structures to enhance surface area, pore accessibility, and functional group density, represents another cutting-edge approach [97,98]. These nano-engineered materials may offer superior performance in terms of adsorption capacity and selectivity, thus addressing the variability in adsorption performance and advancing the design of highly efficient adsorbents. Incorporating such innovative strategies could significantly accelerate progress in this field.

Finally, the economic feasibility and environmental impact of using pyrolytic carbon-based materials for REEs' recovery need to be assessed comprehensively [9,93]. While these materials are generally low-cost and sustainable, the costs associated with their production, regeneration, and disposal, as well as their life-cycle environmental impacts, must be considered. Future research should focus on developing integrated processes that combine REEs' recovery with other waste treatment or resource recovery operations to enhance overall sustainability and economic viability [14,92].

By addressing these challenges and gaps, future studies can advance the development of pyrolytic carbon-based materials as efficient, scalable, and sustainable solutions for the recovery of REEs, contributing to the secure supply of these critical materials and the advancement of green technologies.

9. Conclusions

The adsorption of rare earth elements onto pyrolytic carbon-based materials offers a promising pathway for the recovery and recycling of these critical resources. Through this review, it is evident that various types of activated carbons, biochars, and simpler carbon materials have demonstrated significant potential in adsorbing REEs from aqueous solutions. The high adsorption capacities reported for functionalized lignin-activated carbon and spent coffee-activated carbon highlight the effectiveness of utilizing waste-derived materials and functionalization techniques to enhance adsorption performance.

While synthetic solutions have provided valuable insights into the adsorption capacities and mechanisms, it is crucial for future studies to test these materials with real leachates. Real-world applications involve complex mixtures with competing ions and contaminants, which can significantly influence adsorption efficiency. Understanding how these pyrolytic carbon-based adsorbents perform in such environments will be essential for optimizing their use in industrial applications and ensuring their practical applicability.

This review also underscores the importance of employing various adsorption isotherm and kinetic models to analyze adsorption behavior. Models such as the Langmuir and Freundlich isotherms, along with pseudo-first-order and pseudo-second-order kinetics, have been instrumental in elucidating the adsorption mechanisms and fitting the experimental data. These models not only help in understanding the interactions between adsorbents and adsorbates but also in predicting the performance of the adsorbents in different conditions.

Given the high supply risk and the critical importance of REEs in modern technology, developing efficient and sustainable methods for their recovery is imperative. The use of more readily available and cost-effective carbon materials, as opposed to complex nanomaterials, aligns well with the objectives of resource recovery and sustainability. These materials offer a practical and scalable solution, making them suitable for broader industrial applications.

The integration of pyrolytic carbon-based adsorbents into the recovery process of REEs supports the principles of a circular economy, where materials are reused, recycled, and recovered to create a closed-loop system. By focusing on functionalized and waste-derived carbons, researchers can develop more sustainable and economically viable solutions. This not only addresses the supply risks associated with REEs but also promotes the efficient use of resources, reducing waste and environmental impact. In doing so, we can support the transition to a low-carbon and high-technology economy that is resilient and sustainable.

In conclusion, advancing the research on pyrolytic carbon-based adsorbents for REE recovery, particularly in the context of real leachates and industrial-waste streams, will be crucial for addressing the supply risks associated with these elements. By aligning these efforts with the principles of a circular economy, we can ensure a more sustainable and resilient supply chain for REEs, contributing to a more sustainable future.

Author Contributions: Conceptualization, M.N., M.B., I.M., F.P. and N.L.; methodology, M.N., I.M., F.P. and N.L.; validation, M.B., M.V., I.M., F.P. and N.L.; formal analysis, M.N., M.B., M.V., I.M., F.P. and N.L.; resources, I.M., F.P. and N.L.; data curation, M.N., M.B., M.V., I.M., F.P. and N.L.; writing—original draft preparation, M.N.; writing—review and editing, M.B., M.V., I.M., F.P. and N.L.; visualization, M.N.; supervision, I.M., F.P. and N.L.; project administration, F.P. and N.L.; funding acquisition, M.B., M.V., I.M., F.P. and N.L. All authors have read and agreed to the published version of the manuscript.

Funding: This work received financial support and help from FCT/MCTES (LA/P/0008/2020 DOI 10.54499/LA/P/0008/2020, UIDP/50006/2020 DOI 10.54499/UIDP/50006/2020, and IDB/50006/2020 DOI 10.54499/UIDB/50006/2020), through national funds. This work was further supported by the RObUST project (RObUST-Valorpneu-FCT_NOVA/23-24) and the Inov.Ação Valorpneu award granted by Valorpneu S.A. Miguel Nogueira acknowledges the support given from FCT/MCTES through a PhD grant (doi.org/10.54499/SFRH/BD/147601/2019). Maria Bernardo thanks FCT/MCTES for funding through program DL 57/2016—Norma transitória. Inês Matos thanks FCT/MCTES for contract CEECIND/004431/2022.

Acknowledgments: The authors would like to thank Recipneu, Lda, and Biogoma, Lda for providing the spent tire-rubber samples used in this study. A special acknowledgment is also due to Valorpneu S.A. for its valuable contribution to getting our team in contact with spent-tire rubber suppliers and for supporting the work in the lab. We would also like to acknowledge the use of Large Language Models for assisting with the improvement of English language, grammar, and syntax during the preparation of this manuscript.

Conflicts of Interest: The authors declare no conflicts of interest.

References

1. European Commission. *Study on the Critical Raw Materials for the EU 2023—Final Report*; European Commission: Brussels, Belgium, 2023.
2. USA Department of Energy. *USA Department of Energy Critical Materials Report—2023*; USA Department of Energy: Washington, DC, USA, 2023.
3. Balde, C.P.; Forti, V.; Gray, V.; Kuehr, R.; Stegmann, P. *The Global E-Waste Monitor 2017*; United Nations University (UNU): Bonn, Germany; International Telecommunication Union (ITU): Geneva, Switzerland; International Solid Waste Association (ISWA): Vienna, Austria, 2017; ISBN 9789280845556.
4. Omodara, L.; Pitkäaho, S.; Turpeinen, E.M.; Saavalainen, P.; Oravisjärvi, K.; Keiski, R.L. Recycling and Substitution of Light Rare Earth Elements, Cerium, Lanthanum, Neodymium, and Praseodymium from End-of-Life Applications—A Review. *J. Clean. Prod.* **2019**, *236*, 117573. [CrossRef]
5. European Commission. *Study on the Review of the List of Critical Raw Materials. Non-Critical Raw Materials Factsheets*; European Commission: Brussels, Belgium, 2017; ISBN 978-92-79-47937-3.
6. Balaram, V. Rare Earth Elements: A Review of Applications, Occurrence, Exploration, Analysis, Recycling, and Environmental Impact. *Geosci. Front.* **2019**, *10*, 1285–1303. [CrossRef]
7. Rademaker, J.H.; Kleijn, R.; Yang, Y. Recycling as a Strategy against Rare Earth Element Criticality: A Systemic Evaluation of the Potential Yield of NdFeB Magnet Recycling. *Environ. Sci. Technol.* **2013**, *47*, 10129–10136. [CrossRef]
8. Cardoso, C.E.D.; Almeida, J.C.; Lopes, C.B.; Trindade, T.; Vale, C.; Pereira, E. Recovery of Rare Earth Elements by Carbon-Based Nanomaterials—A Review. *Nanomaterials* **2019**, *9*, 814. [CrossRef] [PubMed]

9. Binnemans, K.; Jones, P.T.; Blanpain, B.; Van Gerven, T.; Yang, Y.; Walton, A.; Buchert, M. Recycling of Rare Earths: A Critical Review. *J. Clean. Prod.* **2013**, *51*, 1–22. [CrossRef]
10. Buchert, M.; Manhart, A.; Bleher, D.; Pingel, D. Recycling Critical Raw Materials from Waste Electronic Equipment. *North Rhine-Westphalia State Agency Nat. Environ. Consum. Prot. Authors* **2012**, *49*, 30–40.
11. Massari, S.; Ruberti, M. Rare Earth Elements as Critical Raw Materials: Focus on International Markets and Future Strategies. *Resour. Policy* **2013**, *38*, 36–43. [CrossRef]
12. Jowitt, S.M.; Werner, T.T.; Weng, Z.; Mudd, G.M. Recycling of the Rare Earth Elements. *Curr. Opin. Green Sustain. Chem.* **2018**, *13*, 1–7. [CrossRef]
13. Balaram, V. Potential Future Alternative Resources for Rare Earth Elements: Opportunities and Challenges. *Minerals* **2023**, *13*, 425. [CrossRef]
14. Nogueira, M.; Matos, I.; Bernardo, M.; Tarelho, L.A.C.; Ferraria, A.M.; Botelho do Rego, A.M.; Fonseca, I.; Lapa, N. Recovery of Rare Earth Elements (Nd3+ and Dy3+) by Using Carbon-Based Adsorbents from Spent Tire Rubber. *Waste Manag.* **2024**, *174*, 451–461. [CrossRef]
15. Iftekhar, S.; Heidari, G.; Amanat, N.; Zare, E.N.; Asif, M.B.; Hassanpour, M.; Lehto, V.P.; Sillanpaa, M. Porous Materials for the Recovery of Rare Earth Elements, Platinum Group Metals, and Other Valuable Metals: A Review. *Environ. Chem. Lett.* **2022**, *20*, 3697–3746. [CrossRef]
16. Jones, I.; Zhu, M.; Zhang, J.; Zhang, Z.; Preciado-Hernandez, J.; Gao, J.; Zhang, D. The Application of Spent Tyre Activated Carbons as Low-Cost Environmental Pollution Adsorbents: A Technical Review. *J. Clean. Prod.* **2021**, *312*, 127566. [CrossRef]
17. Arena, N.; Lee, J.; Clift, R. Life Cycle Assessment of Activated Carbon Production from Coconut Shells. *J. Clean. Prod.* **2016**, *125*, 68–77. [CrossRef]
18. Thompson, K.A.; Shimabuku, K.K.; Kearns, J.P.; Knappe, D.R.U.; Summers, R.S.; Cook, S.M. Environmental Comparison of Biochar and Activated Carbon for Tertiary Wastewater Treatment. *Environ. Sci. Technol.* **2016**, *50*, 11253–11262. [CrossRef] [PubMed]
19. Kumar Mishra, R.; Singh, B.; Acharya, B. A Comprehensive Review on Activated Carbon from Pyrolysis of Lignocellulosic Biomass: An Application for Energy and the Environment. *Carbon Resour. Convers.* **2024**, *7*, 100228. [CrossRef]
20. Heidarinejad, Z.; Dehghani, M.H.; Heidari, M.; Javedan, G.; Ali, I.; Sillanpää, M. Methods for Preparation and Activation of Activated Carbon: A Review. *Environ. Chem. Lett.* **2020**, *18*, 393–415. [CrossRef]
21. Kumar, A.; Saini, K.; Bhaskar, T. Hydochar and Biochar: Production, Physicochemical Properties and Techno-Economic Analysis. *Bioresour. Technol.* **2020**, *310*, 123442. [CrossRef]
22. Wang, K.; Remón, J.; Jiang, Z.; Ding, W. Recent Advances in the Preparation and Application of Biochar Derived from Lignocellulosic Biomass: A Mini Review. *Polymers* **2024**, *16*, 851. [CrossRef]
23. Perreault, L.L.; Giret, S.; Gagnon, M.; Florek, J.; Larivière, D.; Kleitz, F. Functionalization of Mesoporous Carbon Materials for Selective Separation of Lanthanides under Acidic Conditions. *ACS Appl. Mater. Interfaces* **2017**, *9*, 12003–12012. [CrossRef]
24. Marwani, H.M.; Albishri, H.M.; Jalal, T.A.; Soliman, E.M. Study of Isotherm and Kinetic Models of Lanthanum Adsorption on Activated Carbon Loaded with Recently Synthesized Schiff's Base. *Arab. J. Chem.* **2017**, *10*, S1032–S1040. [CrossRef]
25. Gad, H.M.H.; Awwad, N.S. Factors Affecting on the Sorption/Desorption of Eu (III) Using Activated Carbon. *Sep. Sci. Technol.* **2007**, *42*, 3657–3680. [CrossRef]
26. Anastopoulos, I.; Bhatnagar, A.; Lima, E.C. Adsorption of Rare Earth Metals: A Review of Recent Literature. *J. Mol. Liq.* **2016**, *221*, 954–962. [CrossRef]
27. Asadollahzadeh, M.; Torkaman, R.; Torab-Mostaedi, M. Extraction and Separation of Rare Earth Elements by Adsorption Approaches: Current Status and Future Trends. *Sep. Purif. Rev.* **2021**, *50*, 417–444. [CrossRef]
28. Saha, D.; Akkoyunlu, S.D.; Thorpe, R.; Hensley, D.K.; Chen, J. Adsorptive Recovery of Neodymium and Dysprosium in Phosphorous Functionalized Nanoporous Carbon. *J. Environ. Chem. Eng.* **2017**, *5*, 4684–4692. [CrossRef]
29. Alcaraz, L.; Escudero, M.E.; Alguacil, F.J.; Llorente, I.; Urbieta, A.; Fernández, P.; López, F.A. Dysprosium Removal Fromwater Using Active Carbons Obtained from Spent Coffee Ground. *Nanomaterials* **2019**, *9*, 1372. [CrossRef] [PubMed]
30. Qadeer, R. Adsorption of Neodymium Ions on Activated Charcoal from Aqeous Solutions. *J. Radioanal Nucl. Chem.* **2005**, *265*, 377–381. [CrossRef]
31. Zheng, X.; Zhang, Y.; Bian, T.; Zhang, Y.; Li, Z.; Pan, J. Oxidized Carbon Materials Cooperative Construct Ionic Imprinted Cellulose Nanocrystals Films for Efficient Adsorption of Dy(III). *Chem. Eng. J.* **2020**, *381*, 122669. [CrossRef]
32. Komnitsas, K.; Zaharaki, D.; Bartzas, G.; Alevizos, G. Adsorption of Scandium and Neodymium on Biochar Derived after Low-Temperature Pyrolysis of Sawdust. *Minerals* **2017**, *7*, 200. [CrossRef]
33. Smith, Y.R.; Bhattacharyya, D.; Willhard, T.; Misra, M. Adsorption of Aqueous Rare Earth Elements Using Carbon Black Derived from Recycled Tires. *Chem. Eng. J.* **2016**, *296*, 102–111. [CrossRef]
34. Babu, C.M.; Binnemans, K.; Roosen, J. Ethylenediaminetriacetic Acid-Functionalized Activated Carbon for the Adsorption of Rare Earths from Aqueous Solutions. *Ind. Eng. Chem. Res.* **2018**, *57*, 1487–1497. [CrossRef]
35. Chen, S.; Xiao, M.; Lu, D.; Zhan, X. Carbon Nanofibers as Solid-Phase Extraction Adsorbent for the Preconcentration of Trace Rare Earth Elements and Their Determination by Inductively Coupled Plasma Mass Spectrometry. *Anal. Lett.* **2007**, *40*, 2105–2115. [CrossRef]

36. Ramasamy, D.L.; Puhakka, V.; Doshi, B.; Iftekhar, S.; Sillanpää, M. Fabrication of Carbon Nanotubes Reinforced Silica Composites with Improved Rare Earth Elements Adsorption Performance. *Chem. Eng. J.* **2019**, *365*, 291–304. [CrossRef]
37. Haggag, E.S.A.; Embaby, M.A.; El-Sheikh, A.S.; Fathy, N.A.; El-Kady, A.A. High Efficiency Simultaneous Adsorption of Rare Earth Elements from Aqueous Solutions Using Carbon Xerogel-Chitosan Composite. *Int. J. Environ. Anal. Chem.* **2024**. [CrossRef]
38. Younis, A.M.; Kolesnikov, A.V.; Desyatov, A.V. Efficient Removal of La(III) and Nd(III) from Aqueous Solutions Using Carbon Nanoparticles. *Am. J. Anal. Chem.* **2014**, *05*, 1273–1284. [CrossRef]
39. EL-Masry, E.H.; Ibrahim, H.A.; Abdel Moamen, O.A.; Zaher, W.F. Sorption of Some Rare Earth Elements from Aqueous Solutions Using Copolymer/Activated Carbon Composite: Multivariate Optimization Approach. *Adv. Powder Technol.* **2022**, *33*, 103467. [CrossRef]
40. Kano, N.; Pang, M.; Deng, Y.; Imaizumi, H. Adsorption of Rare Earth Elements (REEs) onto Activated Carbon Modified with Potassium Permanganate (KMnO 4). *J. Appl. Solut. Chem. Model.* **2017**, *6*, 51–61. [CrossRef]
41. Gismondi, P.; Kuzmin, A.; Unsworth, C.; Rangan, S.; Khalid, S.; Saha, D. Understanding the Adsorption of Rare-Earth Elements in Oligo-Grafted Mesoporous Carbon. *Langmuir* **2022**, *38*, 203–210. [CrossRef]
42. Sun, Y.; Wang, Q.; Chen, C.; Tan, X.; Wang, X. Interaction between Eu(III) and Graphene Oxide Nanosheets Investigated by Batch and Extended X-Ray Absorption Fine Structure Spectroscopy and by Modeling Techniques. *Environ. Sci. Technol.* **2012**, *46*, 6020–6027. [CrossRef]
43. Kilian, K.; Pyrzyńska, K.; Pęgier, M. Comparative Study of Sc(III) Sorption onto Carbon-Based Materials. *Solvent Extr. Ion Exch.* **2017**, *35*, 450–459. [CrossRef]
44. Saha, D.; Bhasin, V.; Khalid, S.; Smeriglio, N.; Cuka, S.; Bhattacharyya, D.; Rodgers, J.; Panja, P.; Deo, M.; Apple, T. Adsorption of Rare Earth Elements in Carboxylated Mesoporous Carbon. *Sep. Purif. Technol.* **2023**, *314*, 123583. [CrossRef]
45. Pinheiro, R.F.; Grimm, A.; Oliveira, M.L.S.; Vieillard, J.; Silva, L.F.O.; De Brum, I.A.S.; Lima, É.C.; Naushad, M.; Sellaoui, L.; Dotto, G.L.; et al. Adsorptive Behavior of the Rare Earth Elements Ce and La on a Soybean Pod Derived Activated Carbon: Application in Synthetic Solutions, Real Leachate and Mechanistic Insights by Statistical Physics Modeling. *Chem. Eng. J.* **2023**, *471*, 144484. [CrossRef]
46. dos Reis, G.S.; Schnorr, C.E.; Dotto, G.L.; Vieillard, J.; Netto, M.S.; Silva, L.F.O.; De Brum, I.A.S.; Thyrel, M.; Lima, É.C.; Lassi, U. Wood Waste-Based Functionalized Natural Hydrochar for the Effective Removal of Ce(III) Ions from Aqueous Solution. *Environ. Sci. Pollut. Res.* **2023**, *30*, 64067–64077. [CrossRef] [PubMed]
47. He, Q.; Chen, J.; Gan, L.; Gao, M.; Zan, M.; Xiao, Y. Insight into Leaching of Rare Earth and Aluminum from Ion Adsorption Type Rare Earth Ore: Adsorption and Desorption. *J. Rare Earths* **2023**, *41*, 1398–1407. [CrossRef]
48. Yang, X.; Wan, Y.; Zheng, Y.; He, F.; Yu, Z.; Huang, J.; Wang, H.; Ok, Y.S.; Jiang, Y.; Gao, B. Surface Functional Groups of Carbon-Based Adsorbents and Their Roles in the Removal of Heavy Metals from Aqueous Solutions: A Critical Review. *Chem. Eng. J.* **2019**, *366*, 608–621. [CrossRef] [PubMed]
49. Raninga, M.; Mudgal, A.; Patel, V.K.; Patel, J.; Kumar Sinha, M. Modification of Activated Carbon-Based Adsorbent for Removal of Industrial Dyes and Heavy Metals: A Review. *Mater. Today Proc.* **2023**, *77*, 286–294. [CrossRef]
50. Goswami, L.; Kushwaha, A.; Kafle, S.R.; Kim, B.S. Surface Modification of Biochar for Dye Removal from Wastewater. *Catalysts* **2022**, *12*, 817. [CrossRef]
51. Badsha, M.A.H.; Khan, M.; Wu, B.; Kumar, A.; Lo, I.M.C. Role of Surface Functional Groups of Hydrogels in Metal Adsorption: From Performance to Mechanism. *J. Hazard. Mater.* **2021**, *408*, 124463. [CrossRef]
52. Miloudi, W.A.; Oukebdane, K.; Abderrahim, O. Hyper-Branched Phosphonated Polyethyleneimine Composite for the Removal of Samarium(III) Ions from Aqueous Solutions: Effect of Process Parameters. *Desalination Water Treat.* **2023**, *303*, 181–192. [CrossRef]
53. Wang, J. Adsorption of Aqueous Neodymium, Europium, Gadolinium, Terbium, and Yttrium Ions onto NZVI-Montmorillonite: Kinetics, Thermodynamic Mechanism, and the Influence of Coexisting Ions. *Environ. Sci. Pollut. Res.* **2018**, *25*, 33521–33537. [CrossRef]
54. Sazali, N.; Harun, Z.; Sazali, N. A Review on Batch and Column Adsorption of Various Adsorbent Towards the Removal of Heavy Metal. *J. Adv. Res. Fluid Mech. Therm. Sci. J. Homepage* **2020**, *67*, 66–88.
55. Patel, H.; In, C. Comparison of Batch and Fixed Bed Column Adsorption: A Critical Review. *Int. J. Environ. Sci. Technol.* **2021**, *19*, 10409–10426. [CrossRef]
56. Malbenia John, M.; Benettayeb, A.; Belkacem, M.; Ruvimbo Mitchel, C.; Hadj Brahim, M.; Benettayeb, I.; Haddou, B.; Al-Farraj, S.; Alkahtane, A.A.; Ghosh, S.; et al. An Overview on the Key Advantages and Limitations of Batch and Dynamic Modes of Biosorption of Metal Ions. *Chemosphere* **2024**, *357*, 142051. [CrossRef] [PubMed]
57. Brandani, S. Kinetics of Liquid Phase Batch Adsorption Experiments. *Adsorption* **2021**, *27*, 353–368. [CrossRef]
58. Patel, H. Fixed-Bed Column Adsorption Study: A Comprehensive Review. *Appl. Water Sci.* **2019**, *9*, 1–17. [CrossRef]
59. Myers, T.G.; Cabrera-Codony, A.; Valverde, A. On the Development of a Consistent Mathematical Model for Adsorption in a Packed Column (and Why Standard Models Fail). *Int. J. Heat Mass. Transf.* **2023**, *202*, 123660. [CrossRef]
60. Foo, K.Y.; Hameed, B.H. Insights into the Modeling of Adsorption Isotherm Systems. *Chem. Eng. J.* **2010**, *156*, 2–10. [CrossRef]
61. Al-Ghouti, M.A.; Da'ana, D.A. Guidelines for the Use and Interpretation of Adsorption Isotherm Models: A Review. *J. Hazard. Mater.* **2020**, *393*, 122383. [CrossRef]
62. Chen, X.; Hossain, M.F.; Duan, C.; Lu, J.; Tsang, Y.F.; Islam, M.S.; Zhou, Y. Isotherm Models for Adsorption of Heavy Metals from Water—A Review. *Chemosphere* **2022**, *307*, 135545. [CrossRef]

63. Musah, M.; Azeh, Y.; Mathew, J.; Umar, M.; Abdulhamid, Z.; Muhammad, A. Adsorption Kinetics and Isotherm Models: A Review. *Caliphate J. Sci. Technol.* **2022**, *4*, 20–26. [CrossRef]
64. Qiu, H.; Lv, L.; Pan, B.; Zhang, Q.; Zhang, W.; Zhang, Q. Critical Review in Adsorption Kinetic Models. *J. Zhejiang Univ. Sci. A* **2009**, *10*, 716–724. [CrossRef]
65. Revellame, E.D.; Fortela, D.L.; Sharp, W.; Hernandez, R.; Zappi, M.E. Adsorption Kinetic Modeling Using Pseudo-First Order and Pseudo-Second Order Rate Laws: A Review. *Clean. Eng. Technol.* **2020**, *1*, 100032. [CrossRef]
66. Wang, J.; Guo, X. Adsorption Kinetic Models: Physical Meanings, Applications, and Solving Methods. *J. Hazard. Mater.* **2020**, *390*, 122156. [CrossRef] [PubMed]
67. Langmuir, I. The Constitution and Fundamental Properties of Solids and Liquids. II. Liquids. *J. Am. Chem. Soc.* **1917**, *39*, 1848–1906. [CrossRef]
68. Freundlich, H. Über Die Adsorption in Lösungen. *Z. Phys. Chem.* **1907**, *57U*, 385–470. [CrossRef]
69. De Vargas Brião, G.; Ali, M.; Khim, H.; Chu, H.; Hashim, A.; Chu, K.H. The Sips Isotherm Equation: Often Used and Sometimes Misused. *Sep. Sci. Technol.* **2023**, *58*, 884–892. [CrossRef]
70. Tseng, R.L.; Wu, F.C.; Juang, R.S. Characteristics and Applications of the Lagergren's First-Order Equation for Adsorption Kinetics. *J. Taiwan Inst. Chem. Eng.* **2010**, *41*, 661–669. [CrossRef]
71. Ho, Y.S. Review of Second-Order Models for Adsorption Systems. *J. Hazard. Mater.* **2006**, *136*, 681–689. [CrossRef]
72. Tseng, R.L.; Tran, H.N.; Juang, R.S. Revisiting Temperature Effect on the Kinetics of Liquid–Phase Adsorption by the Elovich Equation: A Simple Tool for Checking Data Reliability. *J. Taiwan Inst. Chem. Eng.* **2022**, *136*, 104403. [CrossRef]
73. Debord, J.; Harel, M.; Bollinger, J.C.; Chu, K.H. The Elovich Isotherm Equation: Back to the Roots and New Developments. *Chem. Eng. Sci.* **2022**, *262*, 118012. [CrossRef]
74. Obradovic, B. Guidelines for General Adsorption Kinetics Modeling. *Hem. Ind.* **2020**, *74*, 65–70. [CrossRef]
75. Weber, W.J., Jr.; Morris, J.C. Kinetics of Adsorption on Carbon from Solution. *J. Sanit. Eng. Div.* **1963**, *89*, 31–59. [CrossRef]
76. Shirzad, K.; Viney, C. A Critical Review on Applications of the Avrami Equation beyond Materials Science. *J. R. Soc. Interface* **2023**, *20*, 20230242. [CrossRef] [PubMed]
77. Whitaker, S.; González-López, M.E.; Laureano-Anzaldo, C.M.; Pérez-Fonseca, A.A.; Arellano, M.; Robledo-Ortíz, J.R. A Discussion on Linear and Non-Linear Forms of Thomas Equation for Fixed-Bed Adsorption Column Modeling Discusión Sobre Las Formas Lineal y No-Lineal Del Modelo de Thomas Para El Modelado de Curvas de Ruptura. *Rev. Mex. Ing. Quím.* **2021**, *20*, 875–884. [CrossRef]
78. Thomas, H.C. Heterogeneous Ion Exchange in a Flowing System. *J. Am. Chem. Soc.* **1944**, *66*, 1664–1666. [CrossRef]
79. Chu, K.H.; Hashim, M.A. Comparing Different Versions of the Yoon–Nelson Model in Describing Organic Micropollutant Adsorption within Fixed Bed Adsorbers. *Environ. Sci. Pollut. Res.* **2024**, *31*, 21136–21143. [CrossRef] [PubMed]
80. Yoon, Y.H.; Nelson, J.H. Application of Gas Adsorption Kinetics I. A Theoretical Model for Respirator Cartridge Service Life. *Am. Ind. Hyg. Assoc. J.* **1984**, *45*, 509–516. [CrossRef]
81. Chu, K.H. Breakthrough Curve Analysis by Simplistic Models of Fixed Bed Adsorption: In Defense of the Century-Old Bohart-Adams Model. *Chem. Eng. J.* **2020**, *380*, 122513. [CrossRef]
82. Bohart, G.S.; Adams, E.Q. Some Aspects of the Behavior of Charcoal with Respect to Chlorine. *J. Am. Chem. Soc.* **1920**, *42*, 523–544. [CrossRef]
83. Wang, J.; Guo, X. Adsorption Isotherm Models: Classification, Physical Meaning, Application and Solving Method. *Chemosphere* **2020**, *258*, 127279. [CrossRef]
84. Shan, X.Q.; Lian, J.; Wen, B. Effect of Organic Acids on Adsorption and Desorption of Rare Earth Elements. *Chemosphere* **2002**, *47*, 701–710. [CrossRef]
85. Gao, W.; Wen, D.; Ho, J.C.; Qu, Y. Incorporation of Rare Earth Elements with Transition Metal–Based Materials for Electrocatalysis: A Review for Recent Progress. *Mater. Today Chem.* **2019**, *12*, 266–281. [CrossRef]
86. Liang, Z.; Yin, L.; Yin, H.; Yin, Z.; Du, Y. Rare Earth Element Based Single-Atom Catalysts: Synthesis, Characterization and Applications in Photo/Electro-Catalytic Reactions. *Nanoscale Horiz.* **2021**, *7*, 31–40. [CrossRef] [PubMed]
87. Gong, Z.; Wang, J.; Zhang, K.; Li, B.; Wu, W. Complex Rare-Earth Oxides Leached from the Rare-Earth Concentrate to Prepare the Catalyst for Selective Catalytic Reduction of NO with NH3. *Miner. Eng.* **2020**, *146*, 106135. [CrossRef]
88. El-Khouly, S.M.; Mohamed, G.M.; Fathy, N.A.; Fagal, G.A. Effect of Nanosized CeO_2 or ZnO Loading on Adsorption and Catalytic Properties of Activated Carbon. *Adsorpt. Sci. Technol.* **2017**, *35*, 774–788. [CrossRef]
89. Chu, T.; Xie, M.; Yang, D.; Ming, P.; Li, B.; Zhang, C. Highly Active and Durable Carbon Support Pt-Rare Earth Catalyst for Proton Exchange Membrane Fuel Cell. *Int. J. Hydrogen Energy* **2020**, *45*, 27291–27298. [CrossRef]
90. Yu, Y.; Yu, L.; Koh, K.Y.; Wang, C.; Chen, J.P. Rare-Earth Metal Based Adsorbents for Effective Removal of Arsenic from Water: A Critical Review. *Crit. Rev. Environ. Sci. Technol.* **2018**, *48*, 1127–1164. [CrossRef]
91. Yu, Y.; Zhang, C.; Yang, L.; Paul Chen, J. Cerium Oxide Modified Activated Carbon as an Efficient and Effective Adsorbent for Rapid Uptake of Arsenate and Arsenite: Material Development and Study of Performance and Mechanisms. *Chem. Eng. J.* **2017**, *315*, 630–638. [CrossRef]
92. Chowdhury, N.A.; Deng, S.; Jin, H.; Prodius, D.; Sutherland, J.W.; Nlebedim, I.C. Sustainable Recycling of Rare-Earth Elements from NdFeB Magnet Swarf: Techno-Economic and Environmental Perspectives. *ACS Sustain. Chem. Eng.* **2021**, *9*, 15915–15924. [CrossRef]

93. Jha, M.K.; Kumari, A.; Panda, R.; Rajesh Kumar, J.; Yoo, K.; Lee, J.Y. Review on Hydrometallurgical Recovery of Rare Earth Metals. *Hydrometallurgy* **2016**, *165*, 2–26. [CrossRef]
94. Alam, G.; Ihsanullah, I.; Naushad, M.; Sillanpää, M. Applications of Artificial Intelligence in Water Treatment for Optimization and Automation of Adsorption Processes: Recent Advances and Prospects. *Chem. Eng. J.* **2022**, *427*, 130011. [CrossRef]
95. Mansour, M.; Bassyouni, M.; Abdel-Kader, R.F.; Elhenawy, Y.; Said, L.A.; Abdel-Hamid, S.M.S. Artificial Intelligence for Predicting the Performance of Adsorption Processes in Wastewater Treatment: A Critical Review. In *Engineering Solutions Toward Sustainable Development, Proceedings of the 1st International Conference on Engineering Solutions Toward Sustainable Development, Port Said, Egypt, 2–3 May 2023*; Springer: Berlin/Heidelberg, Germany, 2024; pp. 153–173. [CrossRef]
96. Lakshmi, D.; Akhil, D.; Kartik, A.; Gopinath, K.P.; Arun, J.; Bhatnagar, A.; Rinklebe, J.; Kim, W.; Muthusamy, G. Artificial Intelligence (AI) Applications in Adsorption of Heavy Metals Using Modified Biochar. *Sci. Total Environ.* **2021**, *801*, 149623. [CrossRef] [PubMed]
97. Khan, S.; Naushad, M.; Al-Gheethi, A.; Iqbal, J. Engineered Nanoparticles for Removal of Pollutants from Wastewater: Current Status and Future Prospects of Nanotechnology for Remediation Strategies. *J. Environ. Chem. Eng.* **2021**, *9*, 106160. [CrossRef]
98. Tara, N.; Siddiqui, S.I.; Rathi, G.; Chaudhry, S.A.; Inamuddin; Asiri, A.M. Nano-Engineered Adsorbent for the Removal of Dyes from Water: A Review. *Curr. Anal. Chem.* **2020**, *16*, 14–40. [CrossRef]